Ph.D. Dissertation of Engineering

Inactivation of bacteria and viruses by conventional disinfectant and high-valent copper species in aqueous system: Efficacy and mechanism

수계 내에서 전통적 산화제와 고원자가 구리종을 이용한 박테리아와 바이러스의 불활성화 : 효율과 기작에 관하여

February 2023

Graduate School of Engineering
Seoul National University
Chemical & Biological Engineering

Taewan Kim

Inactivation of bacteria and viruses by conventional disinfectant and high-valent copper species in aqueous system: Efficacy and mechanism

Submitting a Ph.D. Dissertation of
Chemical & Biological Engineering

February 2023

Graduate School of Engineering
Seoul National University
Chemical & Biological Engineering

Taewan Kim

Confirming the Ph.D. Dissertation written by
Taewan Kim
February 2023

Chair	윤 제 용	(Seal)
Vice Chair	이 창 하	(Seal)
Examiner	홍 석 원	(Seal)
Examiner	최 용 주	(Seal)
Examiner	김 민 식	(Seal)

Abstract

Recently, the need for disinfection is continuously increasing due to the outbreak of various pathogens and infection accidents. In particular, the possibility of transmission through water has been raised as the infection routes of specific virus species that spread through the air have diversified, and interest in the inactivation of pathogens in water has greatly increased worldwide. To control pathogens in water, chemical oxidation methods such as chlorine and ozone and photochemical disinfection systems can be applied.

In this study, the inactivation efficiency of various disinfectants and microorganism pairs applied in the disinfection process was quantitatively analyzed, and the inactivation mechanism was investigated. As disinfectants, single anti-oxygen, which is a photochemical disinfectant, chlorine, ozone, and hydrogen peroxide, which are chemical disinfectants, and a copper-based disinfection system were applied. As microorganisms, 8 types of bacteria (including 2 pathogenic types) including *E. coli*, 4 types of bacteriophages, and 2 types of pathogenic viruses (airborne virus) were selected. compared. Additionally, for pathogenic viruses, a study to generalize the inactivation mechanism was additionally performed to show the contribution of inactivation. The main results are as follows.

First, singlet oxygen generated by the photochemical disinfection system shows a linear correlation with the inactivation of microorganisms

and shows high inactivation efficiency in viruses compared to bacteria.

Second, it was confirmed that the similarity of the tendency of microbial inactivation was increased when classified by structural characteristics of microorganisms through the application of a copper-based disinfection system. etc.

Third, it was confirmed that the inactivation of airborne pathogens is easily possible even with the use of existing disinfectants, but the inactivation efficiency is relatively low. In addition, it was confirmed that the inactivation efficiency of microorganisms should be predicted by simultaneously applying changes in the structure by pH, not simply determined by the type and concentration of the oxidant.

Keyword : Disinfection, Inactivation mechanism, Pathogens, Oxidation, Copper-based disinfectant, conventional disinfectant

Student Number : 2020-26493

Table of Contents

Chapter 1. Introduction

1.1. Emergences pathogens and infectious diseases

1.1.1. Recently emerging pathogens

In recent decades, there have been frequent outbreaks of viruses that cause various zoonotic diseases, especially coronaviruses (CoV) such as SARS-CoV, MERS-CoV and SARS-CoV-2 that are transmitted through the respiratory tract. Particularly, the recent outbreak of COVID-19 (CoV infectious disease-19) is an infection caused by SARS-CoV-2, which is of the *coronaviridae* family (Buonerba et al.,2021; Chan et al., 2020; Meleson, 2020). It is a single-stranded RNA (ssRNA) virus 120 nm in size and has a thin lipid layer called envelope. Envelope, which is a distinguishing character of CoV, refers to a structure that is composed of a spherical lipid bilayer membrane enclosing the protein capsid of a virus and RNA, and a crown-like spike composed of proteins or glycoproteins. The structure further improves the infectivity by increasing the binding force between the virus and the host cell and provides an opportunity to be more stable when exposed to an aerosol state (Wang et al.,2020).

In addition, various types of pathogens such as water-borne viruses (e.g., norovirus, rotavirus, etc.) and antibiotic-resistant bacteria continue to be a problem. Waterborne viruses have been a problem for decades. This problem was expected to be solved with the development of water treatment technology, but it still has not reached a complete solution and is causing

suffering to many people. Most of these waterborne viruses are single-stranded RNA viruses and have a size of 200 nm or less. Most of these viruses do not develop structures such as envelopes or spikes and have a life cycle very similar to that of bacteriophages (WHO, 2020; Haramoto et al., 2018; La Rosa et al., 2012; WHO, 2017; Gall et al., 2015; Wiggington et al., 2015; Cui et al., 2019). These characteristics have the potential to cause more frequent outbreaks in high-risk patients who are at risk of developing opportunistic infections. Antibiotic-resistant bacteria refer to bacteria that have genetic information (plasmid) that is resistant to a specific antibiotic among bacteria (Daughton., 2020; Vandermeulen et al.,2011). These super-bacteria have a potential risk of generating new antibiotic-resistant bacteria because they can be treated only through a combination of various antibiotics during infection. For this reason, it has the potential to become a progressively greater threat to the ecosystem over time. Surprisingly, the threat posed by these pathogens has increased markedly in the last decade. Therefore, the demand for the development of technologies that can reliably control these potential threats has gradually increased.

1.1.2. Threats of pathogens in aquatic system

CoV is a respiratory pathogenic virus and basically transmitted by contact through hand-mediated contamination or through respiratory droplets caused by sneezing, coughing, and breathing (Sun et al., 2020; Tang et al., 2020; Wolfel et al., 2020; Zhang et al., 2020). Therefore, most of the

proposals for preventing of CoV infection focused on controlling the rate of infection by adopting methods to protect the respiratory tract and hands, such as sanitizing hands and touching objects or wearing a mask to prevent saliva leaking (Cai et al, 2020; Chan et al., 2020; Chin et al., 2020). Despite these efforts, other potential routes of infection have been suggested. A typical example is the possibility of infection through the ocular surface and the fecal-to-oral routes. Prior to the emergence of SARS-CoV in China in 2002, CoV was considered entirely a respiratory virus (Ahmed et al., 2020; Arora et al., 2020; Balboa et al., 2020; Kocamemi et al., 2020a, 2020b; Kumar et al., 2020; Medema et al., 2020; Meulemans, 1987; Nemudryi et al., 2020; Randazzo et al., 2020; La Rosa et al., 2020; Wurtzer et al., 2020). However, it has been confirmed that SARS-CoV can also affect the human enteric system (Núñez-Delgado, 2020). In general, domestic wastewater can be contaminated with feces or shower/laundry wastewater infected by CoV. Therefore, domestic wastewater is highly likely to be a potential carrier for transmitting viruses. Although recent studies have shown that the infectivity of viruses present in wastewater is scarce persistence, this possibility poses a serious potential hazard to public and personal health due to transmission through aqueous media (Esper et al., 2010; Jevsnik et al., 2013; Risku et al., 2010; Vabret et al., 2006). Although the WEF excluded the possibility of male-mediated transmission as a possible transmission route of SARS-CoV2, it was recognized as a potential transmission route according to various results of studies through the outbreak of MERS and SARS. Even if

the possibility of transmission is remarkably low, a reliable sterilization technique is necessary considering the ripple effect of transmission.

Moreover, both antibiotic-resistant bacteria and waterborne viruses are known to be infected or produced by contaminated water or antibiotic substances remaining in contaminated water. Therefore, it is necessary to develop a technology that can treat pathogens in the water system, leaving aside airborne viruses that have recently emerged and become a threat. In developed countries such as the United States, protozoa such as *Giardia* and *Cryptosporidium* remain as potential infectious agents even though they are sufficiently sterilized in the water treatment process. This is because cysts of protozoa play a role in protecting the body from such adverse conditions. In antibiotic-resistant bacteria, there is a possibility that the thick cell membrane and the envelope structure of a specific virus may play the same role as cysts. Moreover, if the antibiotic-resistant bacteria are Gram-positive, this possibility may increase (Utili, 2001; Jubeh et al., 2020; Fenta et al., 2022; Mamishi et al., 2019). Therefore, for complete inactivation of pathogens in aquatic systems, a deeper understanding of the specific characteristics of pathogens is required.

1.1.3. Classification of the types of microorganisms and its differences

Pathogenic microorganisms can be broadly classified into bacteria,

viruses, and protozoa, each of which can be further subdivided (Chan et al., 2002, Burge et al., 1981; Cai et al., 2011; McGough et al., 1990; Reich et al., 2018). Although the number of infections caused by protozoa has decreased worldwide in recent decades, the number of bacterial and viral infections has continued to increase (Mauck et al., 2012; Beck et al., 2000; Varsani et al., 2008; Duxbury et al., 2019; Mina et al., 2019). Therefore, it is necessary to classify bacteria and viruses in detail and then analyze each characteristic and the difference in inactivation resulting therefrom.

The bacteria are microscopic single-celled organisms. There are thousands of bacteria, and they live everywhere (soil, seawater, etc.). Even in the human body, it reproduces vigorously in all parts of the body, including the skin, oral cavity, digestive tract, and reproductive organs (Halliday and Gast, 2011; Elmir et al., 2007; Whitman et al., 2014; Boulanger et al., 2004; Natsch et al., 2006; Zychowski and Bryndal, 2015). Therefore, among these bacteria, pathogenic individuals need to be actively controlled. Pathogenic bacteria refer to those that continuously produce toxins or penetrate body tissues and cause inflammatory reactions. Some bacteria invade the heart, nervous system, etc., rather than a simple inflammatory reaction, causing serious damage (Pankuweit et al., 2005). There are even studies that some bacteria (e.g., Helicobacter pylori) can cause cancer or other severe infectious disease (Polk et al.,2010; Helgason et al., 2000; Inglesby et al., 2000). Bacteria can be classified in detail based on scientific name, phylogenetic separation, morphology, oxygen need, and

genetic composition. Among them, the factors that can cause changes in the rate or mechanism of inactivation are differences in characteristics according to phylogenetic classification and shape. Phylogenetic classification is judged based on the reaction to a specific dye and is generally classified into Gram-positive bacteria and Gram-negative bacteria according to the reaction to Gram stain (Coico, 2006; Thairu et al., 2014; Magee et al., 1975; Bartholomew and Mittwer, 1952). Both gram-positive and gram-negative bacteria are stained with gram stain, but in the subsequent bleaching process, gram-positive bacteria with a thick peptidoglycan layer are not decolorized, and gram-negative bacteria are decolored (Kim et al., 2015; Schumann 2011; Allen et al., 1987). Therefore, it can be said that Gram-positive bacteria have a thicker cell wall than Gram-negative bacteria and are relatively resistant to oxidative stress. In addition, it can be confirmed that there are bacteria in the form of cocci, spiral bacteria, and spirochetes, and the ratio of each inactivation by the oxidant is significantly different (Mainardi et al., 2008; Wang et al., 2007).

Viruses are microscopic pathogens that parasitize inside other organisms. Since it cannot reproduce on its own, it needs a host, which can infect all living things, including bacteria and animals (Wiggington and Kohn, 2012; Lin et al., 2020; Springthorpe and Sattar, 1990; Mbithi et al., 1990). Viral particles (virions) consist of an envelope that protects genetic material made up of DNA or RNA. The shape of the protein envelope (capsid) has a wide variety of features, from a simple spiral to an oval. The

average virion size is between one-hundredth and one-thousandth that of bacteria. These capsids are polymers of protein beads (capsomers), in which certain viruses additionally possess a lipid envelope. This lipid is derived from the host cell and the virus has separated the cell membrane that the host cell has. Viruses possess a lytic cycle that can destroy host cells. This causes an inflammatory response in the human body and causes various infectious diseases. Viruses are classified by the ICTV (International Committee on Taxonomy of Viruses), the Baltimore Classification, and the Holmes Classification (Mallapity, 2020). Among them, the Baltimore classification is classified according to the type of nucleic acid, strand, pole, and replication method, and has a total of 7 groups. Comparing the correlation between the classification results in the Baltimore classification and UV disinfection, RNA virus is inactivated with higher efficiency than DNA virus, and single-stranded shows higher efficiency than double-stranded. On the other hand, comparative studies on this property in inactivation by oxidative stress have not been sufficiently conducted.

1.2. Disinfection system

1.2.1. Photochemical disinfection system

Photochemical disinfection systems are largely divided into direct disinfection and indirect disinfection methods. Direct disinfection among photochemical disinfection refers to sterilization technology that can directly control pathogens by using ultraviolet (UV) light. UV is the most

effective and economical technology to control pathogens among currently known technologies. Unlike ozone (O_3), which shows disinfection ability based on strong oxidizing power, UV does not decompose other organic pollutants by itself, and shows a specialized performance for sterilization. In general, it has been widely used to control protozoa such as *Cryptosporidium*, but recently it has been widely used for the control of viruses. It is the most suggested disinfection method along with copper and ethanol for the control of CoV, which has recently become a global problem. Unlike other methods, the direct photochemical oxidation method has the advantage of being least affected by chemical factors such as temperature and pH. In addition, there is a disadvantage that there is no residue and there is an advantage that there is no disinfection by-product. UV is light with wavelengths from 100 nm to 400 nm, and each wavelength has different characteristics and roles. In general, the most used wavelength for disinfection is 254 nm UV, which is known to absorb the wavelength of DNA and protein in the corresponding region and absorbs UV of this wavelength to generate a genetic mutation (T-T dimer), As a result, it shows an inactivation mechanism. Recently, a far-UV process using a wavelength of 222 nm is also being actively studied.

In the indirect photochemical disinfection system, the method that utilizes photochemically generated reactive oxygen species has been studied most frequently. Microbial inactivation using reactive oxygen species (ROS) generated by photochemical reactions such as hydroxyl radical ($^{\bullet}OH$) and

singlet oxygen ($^1O_2$) has been studied from the perspective of understanding natural disinfection processes driven by sunlight (Kohn et al., 2007; Cho et al., 2004; Horie et al., 1996; Cho et al., 2010; Mamane et al., 2007; Dahl et al., 1987; Dahl et al.,1989; Dahl et al., 1988) as well as developing alternative disinfection technologies for water and wastewater treatment (Liu et al., 2016; Bezman et al., 1978; Hotze et al., 2009; Müller-Breitkreutz et al.,1995). Different photochemical systems including UV/H_2O_2, UV/TiO_2, UV/C_{60}, Vis/NOM, Vis/MoS_2, and Vis/edible dyes have been tested for the inactivation of *E. coli*, MS2, and *B. subtilis* (Schäfer et al., 2000; Silverman et al., 2013; Ryberg et al., 2018). These studies have also investigated the factors affecting the efficacy of microbial inactivation such as light intensity, pH, temperature, etc. It is known that ROS exert oxidative damages to cell membranes and other intracellular components (Cho et al., 2005; Foster et al., 2011; Castro-Alférez et al., 2016; Amrullah et al., 2019). As it is a more selective oxidant than $^{\bullet}OH$, $^1O_2$ can be more effective in inactivating microorganisms by avoiding undesired consumption through reactions with water constituents (Brame et al., 2014). $^1O_2$ is readily generated by photosensitizers with visible light illumination in the presence of oxygen (Foote et al., 1968a; Foote et al., 1968b). Microbial inactivation by $^1O_2$ has been examined using different visible light-photosensitizers such as organic dyes, metal complexes, and fullerenes (Cho et al., 2010; Dahl et al., 1987; Dahl et al., 1989; Dahl et al., 1988; Bezman et al., 1978; Hotze et al., 2009; Müller- Breitkreutz et al.,1995; Schäfer et al., 2000; Ryberg et al.,

2018). These $^1O_2$-generating systems using visible light-photosensitizers have often been suggested to be applied as solar disinfection technologies for drinking water treatment in underdeveloped countries (Ryberg et al., 2018; Jiménez-Hernández et al.,2006).

1.2.2. Chemical oxidation system

The chemical oxidation is a strong and rapid tool that can inactivate a broad spectrum of microorganisms in water (Dow et al., 2006; Gomes et al., 2016; Møretrø et al., 2012; Shin and Sobsey., 2003; Sobsey, 1989; Sproul et al., 1982). For water disinfection, chemical oxidants such as chlorine, chlorine dioxide, and ozone have been extensively studied and used in water treatment plants (Boudaud et al., 2012; Cho et al., 2006; Cho et al., 2010; Zou et al., 2013). These oxidants are known to damage cell membranes, nucleic acid and mitochondria as well as other cellular components of the microorganisms (Maness et al., 1999; Sproul et al., 1982; Young and Setlow, 2003). However, these conventional disinfectants can produce harmful disinfection by-products by the reactions with natural or anthropogenic organic substances in water (Sohn et al., 2004). Conventional disinfectants generally include chlorine, ozone, and chlorine dioxide, and each has advantages and disadvantages. Chlorination is a disinfectant that has been typically used in water treatment and is known to be effective against most pathogenic microorganisms present in raw water, and has the advantage of

high persistence. On the other hand, the possibility of the generation of disinfection by-products such as trihalomethane is continuously emerging, and the possibility that chlorine-resistant bacteria can be generated under certain conditions has been raised (Luo et al., 2021). In general, there are three methods for chlorination: a method of directly injecting chlorine gas, a method of using hypochlorite, and a method of electrolyzing brine (Venczel et al., 1997). Chlorine injected in each method reacts with water to produce free chlorine and has two different speciation based on pH 7.5. In general, HOCl generated in a low pH region is known to have a higher disinfecting ability, but this disinfection ability may vary due to the characteristics of specific microorganisms (Sobsey et al., 1988).

Ozonation is a widely used oxidant and is also widely used as a disinfectant. Unlike other disinfectants, ozone is oxidized by several complex reactions (Gunten, 2003a). Ozone is an unstable gas with a serious odor. In the water treatment process, gaseous ozone is directly injected or used in a saturated form in aqueous solution. Ozonation is a widely used oxidant and is also widely used as a disinfectant. Unlike other disinfectants, ozone is oxidized by several complex reactions (Gunten, 2003a). Ozone is an unstable gas with a serious odor. In the water treatment process, gaseous ozone is directly injected or used in a saturated form in aqueous solution. Ozone reacts by direct oxidation and indirect oxidation reaction. Direct oxidation is a method in which ozone with an oxidation-reduction potential of 2.07 V directly oxidizes organic matter and microorganisms. 2.80 V) to

sterilize microorganisms. The ozone depletion reaction is accelerated as the pH increases, resulting in more hydroxyl radicals and superoxide radicals. In most cases, this reaction results in higher microbial inactivation efficiency at high pH. Ozone is also known to have a risk of forming bromate, a carcinogenic disinfection by-product under certain conditions (Gunten, 2003b).

1.2.3. Other methods

Attempts to develop various disinfection systems are continuing recently due to the impact of the recent outbreak of the CoV. Conventionally, a method of using a metal surface or metal ions, a method of alkalizing, etc. are widely used. In particular, gases such as ethylene oxide, which act as an alkalizing mechanism, are widely used in medical devices that come in frequent contact with the human body, and various gaseous substances for similar purposes are being developed. Except for heavy metals, metals are generally necessary for all living things. They catalyze the maintenance of various enzymatic functions and metabolic processes and structure formation in cells. However, at high concentrations these metals can cause fatal damage to some living organisms. Therefore, although the antibacterial effect of metals with relatively low toxicity to the human body has been extensively studied, the metal-induced biocidal action is still unclear. Several studies have reported that various metals cause microbial damage by

excessive oxidative damage or binding to proteins or membranes (Dizaj et al., 2014; Lemire et al., 2013). However, the metals most likely to cause such damage are selected as Ag, Fe, or Cu and Zn, which form superoxide dismutase in living organisms. For this reason, recently, research on disinfection systems using metals such as Cu or Ag has been actively conducted. However, Ag is relatively toxic, so Cu is preferred.

Cu is a well-known microbicide that has been widely used to control microorganisms (Borkow and Gabbay, 2004; Crist et al., 1988; Dwidjosiswojo et al., 2011; Ohsumi et al., 1988). Cu ions bind to reactive sites of proteins and DNA in microbial cells, leading to dysfunctions in these biomolecules (Lie et al., 2002; Rajendirn et al., 2007; Vile et al., 1999). Cuprous ion (Cu(I)) is recognized to be more cytotoxic than cupric ion (Cu(II)) (Beswick et al., 1976; Chen et al., 2013; Kirakosyan et al., 2008; Park et al., 2012). The microbicidal effect of exogenous Cu(II) has been suggested to be attributed to the toxicity of Cu(I) reductively generated in the intracellular region (Nguyen et al., 2013). Even in this regard, recent studies are being conducted to produce copper films with antiviral properties.

1.3. Latest research trends

1.3.1. Disinfection system

Recently, research related to the development of a new disinfection system that can be applied to water systems is continuously being conducted, and most of them focus on maximizing the disinfection ability by combining existing disinfection systems. In particular, there is a study that combines a copper-based disinfection system and an oxidation system to produce various copper species and compares the efficacy of each microorganism inactivation. The previous studies demonstrated that the combined use of Cu(II) with hydrogen peroxide (H_2O_2) or hydroxylamine (HA) (or with both of H_2O_2 and HA) significantly enhances the microbicidal activity of Cu(II) (Kim et al., 2015; Lee et al., 2017). The combination of Cu(II) with H_2O_2 (Cu(II)/H_2O_2) generates reactive oxidants such as hydroxyl radical ($^{\bullet}OH$) and cupryl ion (Cu(III)) that can exert oxidative damage to bacterial cells and viral particles (Kim et al., 2015). HA as a reducing agent converts Cu(II) into Cu(I), which further reacts with oxygen to produce different oxidizing species. Hence, the combination of Cu(II) with HA (Cu(II)/HA) generates multiple redox species that exhibit different microbicidal mechanisms towards bacteria and viruses (Kim et al., 2015). In addition, the ternary combination of Cu(II)/HA/H_2O_2 maximized the generation of reactive oxidants. In particular, Cu(III) was found to be a selective virucide (Kim et al., 2015). The Cu(II)/HA and Cu(II)/HA/H_2O_2 systems were also

effective in inactivating bacterial biofilms (Lee et al., 2017). The zero-valent iron-copper nanoparticles can generate Cu(III) in-situ, thereby exhibiting a high disinfection ability compared to the other Cu disinfection system (Kim et al., 2019). In addition, recent studies related to selective inactivation of microorganisms on the surface using oxidizing agents generated by electrochemical and photochemical methods are continuously being conducted (Buonanno et al., 2020).

1.3.2. Inactivation mechanisms

In the current water treatment process, a method for inactivation by applying various disinfection systems with respect to the control of pathogens, which is one of the biggest problems, has been proposed, and is being introduced in water treatment plants. However, it is difficult to say that the inactivation mechanism for each disinfectant and microorganism couples were completely understood because it was designed with a general disinfection ability, not considering the characteristics of the local infectious agent. In general, the mechanism by which a disinfectant inactivates microorganisms is when the disinfectant destroys the outer membrane or wall of microorganisms (Surface disruption), penetrates inside and directly damages organelles or genes that have an important effect on metabolism (Diffusion), In some cases, reproduction is inhibited. Inactivation of microorganisms by oxidants leads to an increase in diffusion caused by

increased membrane permeability after surface disruption in both bacteria and viruses (Kim et al., 1980, Foegeding et al., 1986, Haas and Engelbrecht, 1980). Due to these characteristics, most studies attempted to elucidate the inactivation mechanism using livedead baclight assay, which is an indicator of microbial surface destruction, but it was not fully explained. Since the chemical characteristics (e.g. surface affinity, binding energy, etc.) of each substructure of the microorganisms were not considered, detailed explanations were lacking. Therefore, various molecular biological attempts have been applied recently to understand the inactivation mechanism.

In the case of using qPCR, a molecular biological method that has been attempted recently, damage to a gene can be identified, and microbial surface destruction can be confirmed through decomposition of lipids or proteins contained in the microbial membranes or wall. Additionally, damage to the cell wall or membrane can be further identified through staining methods. In accordance with the technological progress of the last decade, most of the research on microbial inactivation uses molecular biological diagnostic equipment such as qPCR and informs about the correlation between gene damage and microbial inactivation (Kim et al., 2019, Wang et al., 2020, Buonerba et al., 2021). Studies on the decomposition of lipids, proteins, and polysaccharides, which are components that make up the surface of microorganisms, are also being actively conducted, and studies are sometimes conducted to check the oxidation pathways of amino acids in detail using LC/MS (How et al., 2014,

Bednarski et al., 2020).

1.3.3. Limitation

As identified in the latest research trends, new disinfection systems are continuously being developed in recent years, and attempts are being made to identify the mechanism of microbial inactivation by molecular biological methods. However, additional research is required on the part that there was no attempt to generalize the inactivation mechanism of microorganisms despite various recent studies, and the lack of identification of disinfectants optimized for each pathogen and evaluation of disinfection performance.

1.4. Purpose of Research

The risks from pathogenic microorganisms are always present in aquatic systems. The probability of finding infectious pathogens, especially viruses, after the water treatment process was extremely rare. This is because the probability of the presence of viruses in water resources is low, and disinfection processes such as chlorination or ozonation are always in operation in the water treatment process. However, there is a low probability that pathogenic viruses will be found in water intake sources adjacent to i) where pathogenic wastewater is discharged, and ii) where water recycling is likely to occur. Therefore, it is necessary to apply the type and concentration

of the disinfectant suitable for the characteristics of the microorganism in consideration of the type of the released pathogen, the type of the disinfectant, and the characteristics of the raw water. In order to apply a disinfectant suitable for the characteristics of microorganisms, it is necessary to identify the kinetics and mechanism of inactivation. Therefore, in this study, the following research goals were set below. All research progresses were carried out sequentially to achieve the final goal (investigation of a disinfection system suitable for inactivation of pathogenic microorganisms).

- To investigate the kinetic characteristics and highly reactive active sites of each disinfection system through the application of various disinfection systems (Chapter 3-5)

This study aimed to evaluate the efficacy of inactivation of bacterial and viral species by various active oxidizing species. For this purpose, conventional disinfectants and new types of disinfectants such as 102 and Cu(III) were applied to inactivation of various bacteria and viruses to confirm the inactivation efficiency and mechanism. Bacteria and virus species were selected as representative species with different types of active sites.

- To investigate the correlation between classification and inactivation

efficacy of microorganisms through application to various types of microorganisms (Chapter 4)

The aim of this study was to evaluate the inactivation efficacy of various bacterial and viral species by Cu(II)/H_2O_2, Cu(II)/HA and Cu(II)/HA/H_2O_2 systems and to evaluate the differential sterilization applied to target microorganisms. to understand the effect. For this purpose, 12 different bacteria and viruses (including gram-negative and gram-positive bacteria, RNA and DNA viruses, mostly non-pathogenic surrogates, with the exception of *S. pneumoiae and S. Aureus*) were selected for inactivation experiments. The inactivation efficacy of selected microorganisms was evaluated in Cu(II)/H_2O_2, Cu(II)/HA and Cu(II)/HA/ H_2O_2 systems. Protein oxidation and nucleic acid disruption were quantified for inactivated microorganisms.

- To elucidate the inacitvation mechanisms by oxidant through direct application to pathogens (Chapter 5)

This study aims to investigate the inactivation efficiency and mechanism of pathogenic viruses by various conventional disinfectants. In particular, a detailed study was conducted on the inactivation efficiency of airborne viruses, which has recently become a problem, in aqueous systems. To this end, CoV and AdV inactivation experiments were performed by varying the

concentrations of each conventional disinfectant under tris buffer conditions. In addition, to confirm the change in inactivation efficiency in natural water, inactivation in various pH ranges that may exist in natural water was confirmed. Additionally, to confirm the mechanism of virus inactivation, the correlation with the degradation of lipids, proteins, and genetic materials was investigated to determine which sites were vulnerable to the attack of disinfectants, and detailed mechanisms were identified.

Chapter 2. Materials & Methods

2.1. Reagents

All chemicals used in this study were of reagent grade and were used without further purification. Agar, nutrient broth, tryptone, yeast extract and tryptic soy broth, sterilized Dulbecco's modified eagle's medium (DMEM) for microbial cultivation and tris buffer for experiments were purchased from Becton Dickinson Co. Rose Bengal dye (RB), furfuryl acid (FFA), copper sulfate, hydroxylamine solution (50 wt%), hydrogen peroxide solution (30 wt%), sodium chloride (NaCl), D-(+)-glucose, calcium chloride ($CaCl_2$), perchloric acid, sodium thiosulfate, ethylenediaminetetraacetic acid (EDTA), and sodium hydroxide were purchased from Sigma-Aldrich Co. All solutions were prepared using deionized Milli-Q water (>18 MΩ·cm, Millipore Co.) and were stored at 4˚C. All glassware was sterilized prior to use by autoclaving at 121˚C for 15 min. The stock solution of O_3 was prepared in a reactor arranged in cooling system by sparging the O_3 gas generated in the O_3 generator (OzoneTech Lab-II) in DI water until it reached a saturated concentration (>20 mg/L). The oxidants were used after quantifying the concentration by a direct measurement method using a UV/Vis spectrophotometer before use.

2.2. Culture and analysis of microorganisms

The type strains of five Gram-negative bacteria (*E. coli* (ATCC 8739), *V. harveyi* (ATCC BAA-1116), *S. flexneri* (ATCC 29903), *S. typhimurium* (ATCC 14028) and *P. aeruginosa* (ATCC 700829)), three Gram-positive bacteria (*B. Subtilis* (ATCC 6633), *S. Aureus* (ATCC 12600) and *S. pneumoniae* (ATCC BAA-334) and four viruses (MS2 (ATCC 15597-B2), T1 (ATCC 11303-B1), T4 (ATCC 11303-B4), and T7 (ATCC 11303-B7) bacteriophages) were selected as surrogate microorganisms for the experiment. Bacteria cells were inoculated in 30 mL of medium (Difco nutrient broth for *E. coli*, Nutrient broth+1.5% NaCl for *B. subtilis* and *S. Aureus*, Tryptic soy broth+ 2% NaCl for *V. harveyi*, Tryptic soy broth for other bacterial cells). The cells were grown at 37˚C for 18–24 h, except for *V. harveyi* (grown at 25˚C). The cells were harvested by centrifugation at 3000 g for 15 min and were washed at least 3 times with 30 mL phosphate buffered solution (PBS, 10 mM, pH 7.2). The bacteria stock suspensions (~10^9 CFU/mL) were prepared by resuspending the cells in 20 mL PBS and were stored at 4˚C until use. The spread plate method (using appropriate agar plates) was used to determine the cell population in the samples (undiluted and serially diluted). After spreading, the plates were grown in an incubator at 37˚C for 18–24 h, and then the numbers of cell colonies were counted.

Viral particles were grown with its host bacteria (*E. coli* ATCC 15597

for MS2 bacteriophage and 11303 for T series bacteriophage). The host *E. coli* cells were inoculated in LB broth containing 10 g/L tryptone, 1 g/L yeast extract, 8 g/L NaCl, 2 mM $CaCl_2$, 1 g/L glucose, and 0.01 g/L thiamine ($CaCl_2$, glucose, and thiamine were added after autoclaving) and were grown at 37˚C for 18–24 h under vigorous shaking (120 rpm). Viral particles were grown in the host *E. coli* stock solution for 18–24 h at 37˚C without shaking. Subsequently, viruses were separated from the host *E. coli* cells via centrifugation at 3000 g for 15 min, and the supernatant was filtered with a 0.22 μm PTFE syringe filter to remove the cell debris of the host bacteria. The stock solution of viruses so produced contains ~10^{10} PFU/mL of viral particles. The plaque assay method was employed to determine the population of the viruses in the samples (undiluted and serially diluted) (APHA, 2005). At least duplicated plates were used to analyze the microorganism population.

The type strains of viruses (CoV (NL63) and AdV (Adenovirus 40)) were selected as surrogate pathogenic airborne virus such as SARS-CoV-2 for experiment. The viruses obtained from ATCC and maintained with DMEM solution. The host cell lines (Vero-E6 cell for CoV and A549 epithelial cell for AdV, respectively) were inoculated in DMEM agar and incubated at least 2 days under CO_2 atmosphere. The viral stock solutions which diluted with DMEM solution vortexed vigorously and added to a host monolayer. The viruses were incubated at 37˚C for 2 days. Infected host cell lines were harvested for preparation of stock solution by freezing and

thawing. The solution was extracted with by chloroform method by shaking vigorously and purified. The detailed purification method is described elsewhere.

For quantification of virus concentration, plaque assay method was applied. The cell line was cultured to a concentration of 10^7 cells/wells the day before virus inoculation. A serially diluted virus sample aliquots were inoculated into the cultured cell line. The mixture was sufficiently mixed and stood for 1 h in a CO_2 incubator for sufficiently infect. After infection, removing the sample aliquots, DMEM and 1.5% agar were mixed 1:1 ratio, and 3 mL of each was injected into each well. The well incubated under 37 ˚C for 24 h (5% CO_2 condition). After incubation, well was staining with 3 mL of 0.5% crystal violet solution, plaques were counted after 1 hour to quantify the concentration.

2.3. Inactivation experiments

2.3.1. photochemical experiments

All of the photochemical experiments were performed in a quartz reactor with 50 mL of reaction solution under vigorous stirring at room temperature (24 ± 1˚C). The reaction solution contains either RB and microorganisms (~10^7 CFU or PFU/mL) or other reagents such as FFA (100 μM) in order to measure $^1O_2$ and histidine for $^1O_2$ scavenging. The initial pH of the reaction solution was adjusted using phosphate buffer (10 mM); no significant

variations in pH values were observed during the reaction. The reaction was initiated by illuminating light from a 150 W xenon arc lamp (LS 150, Abet Technologies Inc.) equipped with an AM 1.5 G filter and a 400 nm long pass filter. Aliquots of the samples (1 mL) were withdrawn from the reaction solution at predetermined time intervals, and these were then analyzed to count the numbers of viable cells (or viral particles) following serial dilution with PBS. For the experiments with FFA, the residual concentrations of FFA in the samples were analyzed. All of the experiments were replicated at least three times; averages and standard deviations (error bars) are presented.

For the experiments requiring anoxic conditions, the reactor with the light source was placed inside a N_2 chamber, and the reaction solution was continuously sparged with ultrapure N_2 gas at a flow rate of 0.5 mL/min. The intensity of the incident light was varied between 50, 100, and 200 mW/cm^2 by adjusting the distance between the reactor and the light source.

2.3.2. Inactivation experiments for copper-based oxidation system

Experiments for chapter 4 were performed using a sterilized 60 mL Pyrex flasks with 50 mL of reaction solution open to the atmosphere under vigorous stirring at room temperature (22 ± 1˚C). The reaction solution containing microorganisms (~10^7 CFU or PFU/mL) was adjusted to pH = 7.1 with 0.1 N NaOH and $HClO_4$ without buffers. The pH variation after the

reaction was less than ±0.2. For experiments needing anoxic conditions, the reaction solution was purged for 30 minutes or more using pure nitrogen gas before the experiment. Microbial inactivation was initiated by adding the microbicides (and other reagents when necessary) into the reactor under vigorous mixing (700 rpm); the input concentrations of Cu(II), HA, and H_2O_2 were 5 μM, 10 μM, and 10 μM, respectively. Samples (1 mL) were withdrawn at a pre-determined time, immediately mixed with EDTA and sodium thiosulfate, and serially diluted with PBS to quench the reaction. The samples were assayed on agar plates to count the viable cells or viral particles (Kim et al., 2019; Park et al., 2015). At least, duplicate experiments were conducted, and the average values with the standard deviations were presented.

2.3.3. Pathogenic virus inactivation experiments

All experiments for chapter 5 were performed at room temperature (20±1˚C) using sterilized 50 mL Pyrex reactor sealed with lid with 30 mL of the reaction solution with vigorous stirring. The experimental solution containing viral particles (~10^7 PFU/mL) was adjusted to each pH range for the experiment with tris buffer. The pH change after the reaction was negligible. Viral inactivation was initiated by adding a stock solution of oxidant to the reactor under vigorous mixing (600 rpm). A sample (1 mL) was withdrawn at a predetermined time intervals and immediately mixed

with 100 mM sodium thiosulfate solution (20 μL) and serially diluted with sterile tris buffer to quench the reaction and stored at 4 ˚C before analysis. The infectivity of samples was analyzed on agar plates to count infectious virus particles. At least triplicate experiments were performed and the mean value with standard deviation was presented.

2.4. Quantification of oxidants concentration

2.4.1. Quantification of $^1O_2$ concentration

The steady-state concentration of $^1O_2$ ($[^1O_2]_{ss}$) was calculated using the decomposition kinetics of the probe compound (FFA). The decomposition of FFA during the reaction exhibited pseudo-first order kinetics, expressed as follows in Equation 1.

$$-\frac{d[FFA]}{dt} = k_{obs}[FFA] = k[^1O_2]_{ss}[FFA] \quad (1)$$

where k_{obs} is the observed pseudo-first order rate constant for the FFA decomposition and k is the second order rate constant for the reaction of FFA with $^1O_2$ ($k = 1.2 \times 10^8\ M^{-1}\ s^{-1}$) (Scully et al., 1987). The concentration of FFA during the reaction was monitored over time, and the k_{obs} value was obtained from the slope of the linear plot of $\ln([FFA]_0/[FFA])$ versus time. $[^1O_2]_{ss}$ was then calculated using Equation 2.

$$[^1O_2]_{ss} = k_{obs}/k \quad (2)$$

The concentration of FFA was measured using high performance liquid chromatography (HPLC, Ultimate™ 3000, Dionex Co.) with UV

absorbance detection at 219 nm. Separation was conducted on a ZORBAX Eclipse XDB-C18 column (5 μm, 150 mm x 4.6 mm, Agilent Co.). An 80:20 mixture of phosphoric acid (0.1%v/v) solution:acetonitrile was used as mobile phase at a flow rate of 1 mL/min.

2.5. Kinetic models for microbial inactivation

Kinetic models were used to interpret the inactivation kinetics of *E. coli* and MS2 by $^1O_2$. The Chick-Watson model (Equation 3) (Kouame and Haas., 1991; Hunt and Mariñas., 1997) was applied to the inactivation of MS2.

$$-\mathrm{Log}(N/N_0) \propto Ct \qquad (3)$$

where N and N_0 are the numbers of viable cells (or viral particles) at times t and 0, respectively, *C* is the concentration of disinfectant ($[^1O_2]_{ss}$ in this study), and *t* is the reaction time.

Unlike the inactivation of MS2, the inactivation curves of *E. coli* showed an initial lag phase. Therefore, the delayed Chick-Watson model (Equation 4) (Rennecker et al., 1999) was applied to the inactivation of *E. coli*.

$$-\mathrm{Log}(N/N_0) = 0 \text{ (for } Ct < b), -\mathrm{Log}(N/N_0) \propto Ct \text{ (for } Ct \geq b) \qquad (4)$$

where b is the lag coefficient.

2.6. Analyses of protein, lipid oxidation, and qPCR

A quantitative polymerase chain reaction (qPCR) analysis was performed to quantify the nucleotide damage on RNA (bacterial 16S

ribosomal RNA (rRNA) and viral RNA (for MS2) and DNA (for T-series bacteriophages)) in treated and untreated microorganisms. Nucleotides were extracted from the sampled aliquots of bacteria and virus with the QIAamp® DNA mini kit and Viral RNA mini kit (QIAGEN, Germany), respectively, according to the provided instructions. The qPCR signals were obtained on a CFX96 RT-PCR system (Bio-Rad, USA). Further details of the qPCR analysis are described elsewhere (Kim et al., 2019).

For the amplification of genes (16S rRNA, viral RNA and DNA), primers were designed the same as universal primers for the target microorganisms. The samples for the qPCR analysis contain 2 μL of extracted nucleotide sample aliquot, 250 nM of forward and reverse primers, and 10 μL of SYBR Green dye (as an RNA binding fluorescent dye). The total volume of the sample was summed up to 20 μL by adding nuclease-free water. The qPCR analysis was initiated by the denaturation step at 95°C for 3 min. Then three steps of denaturation (95°C for 15 s), annealing (60°C for 15 s), and extension (72°C for 30 s), were repeated for 40 cycles. While the target RNA is amplified as a function of the repeated cycle, the fluorescence intensity of the sample was measured in real time, and the number of cycles was determined at a specific fluorescence intensity. The amount of RNA in the sample was quantified by the determined number of cycles reaching the specific fluorescence intensity. The standard curve for each nucleotide was prepared using the nucleotide extracted from untreated microorganisms.

To evaluate the oxidation of proteins in microorganisms, OxiSelect™ protein carbonyl fluorophore kits (Cell Biolabs Co.) were used. Proteins in the samples were extracted and stained with a protein carbonyl fluorophore according to the provided instructions. The fluorescence emission at 530 nm (excitation at 480 nm) was measured by a microplate reader (Infinite 200, Tecan Co.) for quantification. The total protein concentration was measured by the value of untreated microorganisms.

For the analysis of lipid oxidation, MDA production was quantified according to the lipid oxidation assay kit (MAK085, Sigma-Aldrich.) and accompanying manufacturer's protocol. After experiment, the sample aliquots were extracted in 250 μL of RIPA buffer and centrifuged at 12,000 xg for 5 min at 4°C. The supernatant was measured with a microplate reader (excitation at 532 nm and emission at 553 nm). MDA values were normalized to total cellular protein content.

Chapter 3. Inactivation of *Escherichia coli* and MS2 coliphage via singlet oxygen generated by homogeneous photosensitization

3.1. Role of $^1O_2$ in microbial inactivation by the Vis/RB system

The Vis/RB system was examined for the inactivation of *E. coli* and MS2 (Figs. 3.1a and 1b, respectively), as well as for the decomposition of FFA (Fig. 3.1c). Control experiments with either light illumination or RB alone did not inactivate microorganisms. Under those conditions, the decomposition of FFA was also negligible. In the absence of oxygen (anoxic conditions), the microbial inactivation by the Vis/RB system was minor; *E. coli* and MS2 were inactivated by 0.7 log in 150 min and 0.6 log in 30 min, respectively. In addition, the decomposition of FFA was negligible in the Vis/RB system under anoxic conditions, indicating that $^1O_2$ was not generated. The minor microbial inactivation by the Vis/RB system under anoxic conditions appears to be caused by the interaction of photoexcited RB with cells (or viral particles). In the condition of irradiating only light, high-intensity light (200 mW/cm$^{2)}$ was irradiated, and a higher concentration (100 μM) was applied even in the system where only RB existed.

The Vis/RB system in the presence of oxygen showed significantly inactivated *E. coli* and MS2 (Figs. 3.1a and 1b) with a noticeable decomposition of FFA (Fig. 3.1c), indicating that the Vis/RB system

generates microbicidal $^1O_2$ by photosensitization. The Vis/RB system showed greater inactivation of MS2 than *E. coli*; *E. coli* and MS2 were inactivated by 4.5 log in 150 min and 3.8 log in 30 min, respectively. The inactivation curve of *E. coli* exhibited an initial lag phase. FFA was completely decomposed in 15 min, following pseudo-first order kinetics. According to the observed decay rate constant of FFA and using Equations 1 and 2, the steady-state concentration of $^1O_2$ was calculated to be 43 pM. When an excess amount of L-histidine (20 mM) as an $^1O_2$ scavenger was added into the system, the decomposition of FFA and microbial inactivation were greatly inhibited, confirming that $^1O_2$ is the responsible microbicidal species.

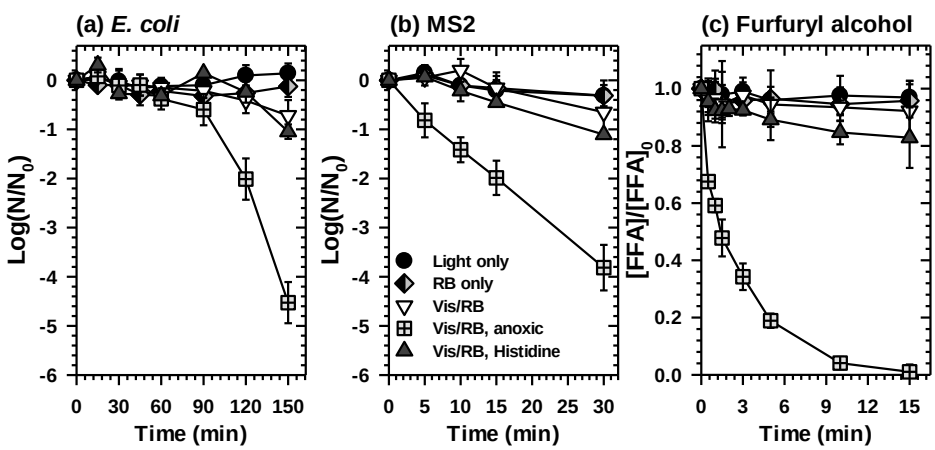

Fig. 3. 1. Inactivation of *E. coli* (a) and MS2 coliphage (b) and decomposition of FFA under different experimental conditions ([*E. coli*]$_0$ = ~10^7 CFU/mL for (a); [MS2]$_0$ = ~10^7 PFU/mL for (b); [FFA]$_0$ = 100 μM for (c); [Histidine]$_0$ = 20 mM; pH = 7.1; unless specified otherwise, light intensity = 100 mW/cm^2, [RB] = 50 μM).

3.2. Effects of RB concentration and light intensity

The inactivation of *E. coli* and MS2 by the Vis/RB system was examined with varying concentrations of RB ranging from 20 to 100 μM (Figs. 3.2a and 2b). Overall, the microbial inactivation was not significantly affected by the concentration of RB; only a slight enhancement was observed at higher RB concentrations. The $[^1O_2]_{ss}$ values calculated from the kinetics of FFA decomposition did not show substantial variations at different concentrations of RB (Fig. 3.2c). The minor influence of RB concentration indicates that the light absorption by RB is nearly saturated at these ranges of concentrations.

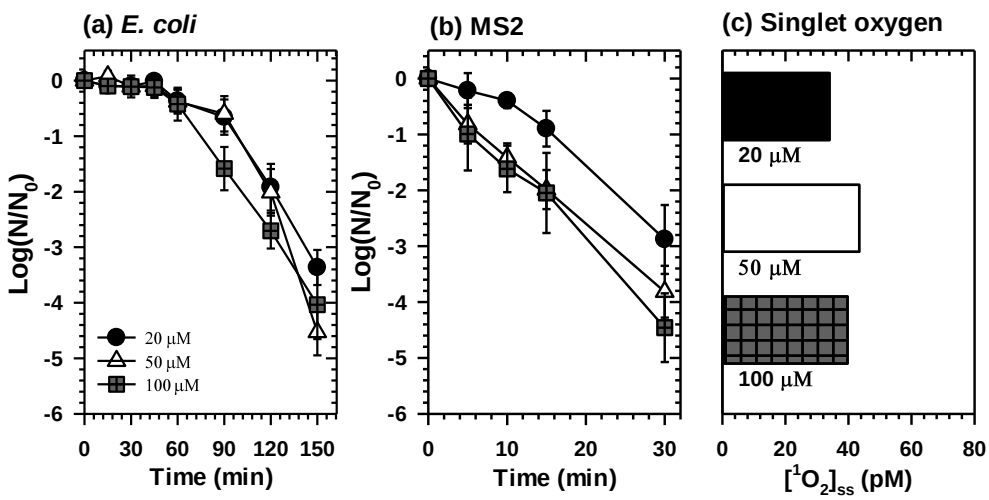

Fig. 3. 2. Inactivation of *E. coli* (a) and MS2 coliphage (b), and the steady-state concentration of $^1O_2$ in the Vis/RB system at different concentrations of RB ($[E.\ coli]_0$ = ~10^7 CFU/mL for (a); $[MS2]_0$ = ~10^7 PFU/mL for (b); $[FFA]_0$ = 100 μM for (c); pH = 7.1; light intensity = 100 mW/cm^2).

The effect of light intensity on the inactivation of *E. coli* and MS2 by the Vis/RB system was examined as well (Figs. 3.3a and 3b, respectively). The results indicated that the microbial inactivation was accelerated with increasing incident light intensity. The inactivation efficacy of *E. coli* was enhanced from 2.1 log inactivation in 150 min at 50 mW/cm^2 radiance to 3.9 log inactivation in 90 min at 200 mW/cm^2 radiance. The inactivation efficacy of MS2 was enhanced from 2.2 log inactivation in 30 min at 50 mW/cm^2 radiance to 3.9 log inactivation in 15 min at 200 mW/cm^2 radiance. The $[^1O_2]_{ss}$ value also increased with increasing light intensity (Fig. 3.3c), showing almost a linear increase with the light intensity. The increased generation of microbicidal $^1O_2$ at higher light intensity is responsible for the enhanced microbial inactivation.

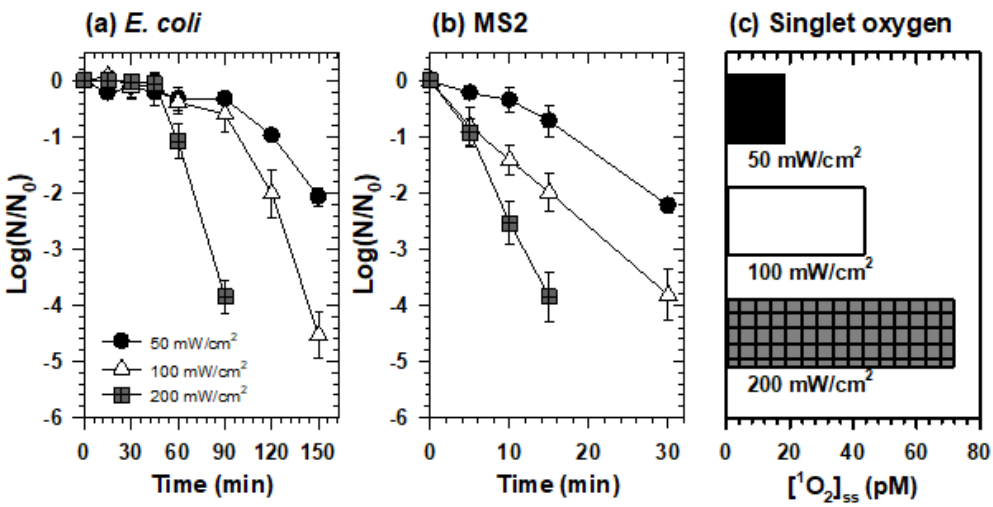

Fig. 3. 3. Inactivation of *E. coli* (a) and MS2 coliphage (b), and the steady-state concentration of $^1O_2$ in the Vis/RB system at different light intensities ([*E. coli*]$_0$ = ~10^7

CFU/mL for (a); $[MS2]_0$ = ~10^7 PFU/mL for (b); $[FFA]_0$ = 100 μM for (c); pH = 7.1; [RB] = 50 μM).

3.3. Effect of pH

The inactivation of *E. coli* and MS2 by the Vis/RB system was examined at different pH values ranging from 5.7 to 8.2 (Figs. 3.4a and 4b). The inactivation efficacy of *E. coli* was considerably higher at pH 5.7 than those at pH 7.1 and 8.2 (Fig. 3.4a). However, the inactivation efficacies of MS2 did not show large differences depending on pH (Fig. 3.4b). The $[^1O_2]_{ss}$ values almost remained constant, regardless of pH (Fig. 3.4c), indicating that the greater inactivation of *E. coli* at pH 5.7 is not caused by the higher yield of $^1O_2$. Similar results were obtained by a previous study (Schäfer et al.,2000) showing that the inactivation rate of *E. coli* at pH 4.5 was approximately 8-fold higher than that at pH 7.0 in the RB-photosensitized system at 25°C, while the generation of $^1O_2$ was not pH-dependent. No clear explanation is currently available for the enhanced inactivation of *E. coli* and MS2 by the Vis/RB system at lower pH values. However, the change in pH may disturb the transport system of the cell membranes, facilitating the penetration of RB or $^1O_2$ into the cell inside (Schäfer et al., 2000, Müller and Engel., 1999).

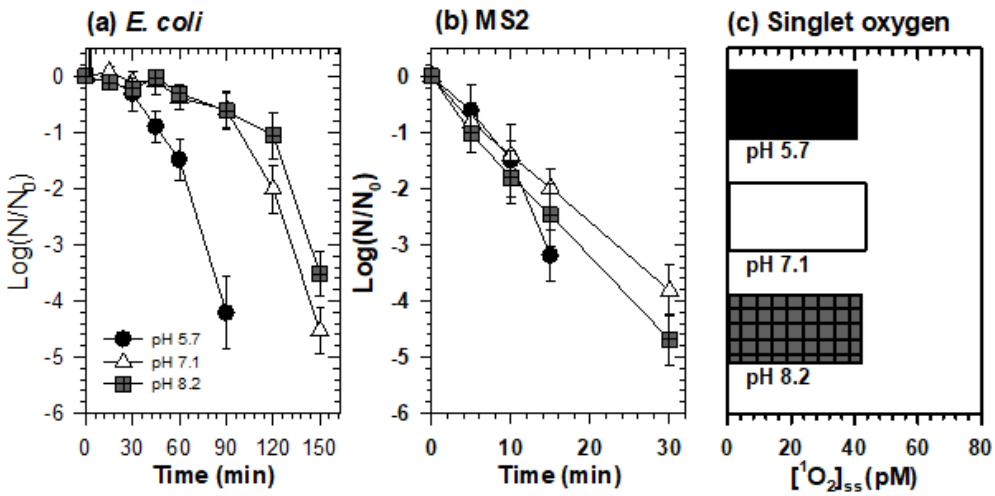

Fig. 3. 4. Inactivation of *E. coli* (a) and MS2 coliphage (b), and the steady-state concentration of $^1O_2$ in the Vis/RB system at different pH values ([*E. coli*]$_0$ = ~10^7 CFU/mL for (a); [MS2]$_0$ = ~10^7 PFU/mL for (b); [FFA]$_0$ = 100 μM for (c); light intensity = 100 mW/cm^2; [RB] = 50 μM).

3.4. Kinetic modeling of microbial inactivation

Using the data on microbial inactivation and $[^1O_2]_{ss}$ in Figs. 3.2–4, the degrees of log inactivation of *E. coli* and MS2 were plotted as functions of *Ct* (concentration-time product, i.e., $[^1O_2]_{ss}t$) (Figs. 3.5a and 5b, respectively); all of the data points in Figs. 3.2–4 were used in the plot, except for those of the *E. coli* inactivation at pH 5.7, which showed a substantial deviation from the $[^1O_2]_{ss}$ trend.

The *Ct* plot of *E. coli* inactivation exhibited a clearer shoulder (the initial lag phase) (Fig. 3.5a), which is consistent with previous observations (Cho et al., 2004). The lag phase in the inactivation curve of *E. coli* has often

been observed for other oxidizing disinfectants such as $^{\bullet}OH$, free chlorine, and chlorine dioxide (Cho et al., 2004, Mamane et al., 2007, Kouame and Haas., 1991, Hunt and Mariñas., 1997). The cell membranes of *E. coli* can serve as barriers protecting the intracellular components from attacks by oxidants. Gram-negative bacteria such as *E. coli* (which have an outer cell membrane) showed larger lag phases than Gram-positive bacteria in the inactivation curves by $^1O_2$ (Schäfer et al., 2000). The delayed Chick-Watson model (Equation 4) was applied to fit the kinetics of *E. coli* inactivation. The lag coefficient (b) and inactivation rate in the subsequent linear phase (the slope of the linear regression curve) were determined to be 5.2×10^{-4} mg·min/L and 2.7×10^4 log inactivation/(mg·min/L), respectively (Fig. 3.5a). The *Ct* value of $^1O_2$ required for the 2-log inactivation of *E. coli* was found to be 1.3×10^{-4} mg·min/L.

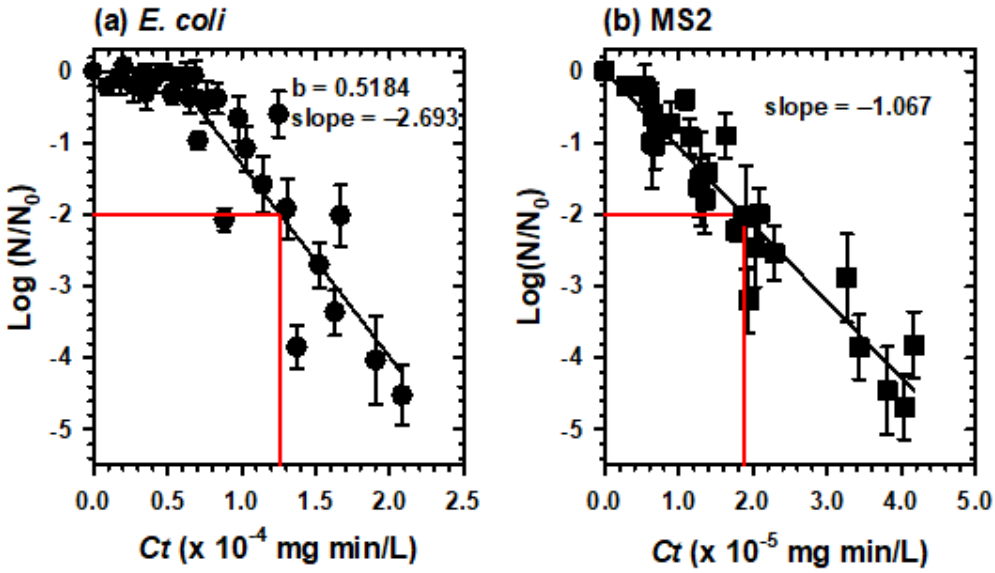

Fig. 3. 5. Inactivation of E. coli (a) and MS2 (b) as a function of Ct. Symbols and lines represent the experimental data points and regression curves according to the (delayed) Chick-Watson model, respectively.

Table 1. *Ct* values required to achieve 2 log microbial inactivation (pH 7.1, buffered condition)

	Disinfectant		*Ct* value [mg min/L]	Reference
E. coli	Chlorine		1.7×10^{-1}	Kouame et al., 1991 Cho et al., 2010
	Chlorine dioxide		$6.0–8.0 \times 10^{-2}$	Cho et al., 2010 Cho et al., 2004
	O_3		$4.0–4.2 \times 10^{-3}$	Hunt and Mariñas., 1997 Cho et al., 2010
	Hydroxyl radical	UV/TiO_2	8.0×10^{-6}	Cho et al., 2004
		UV/H_2O_2	4.5×10^{-9}	Mamane et al., 2007
	Singlet oxygen		1.3×10^{-4}	This study
MS2 coliphage	Chlorine		1.4×10^{-1}	Cho et al., 2005
	Chlorine dioxide		1.7×10^{-1}	Cho et al., 2005
	Hydroxyl radical	UV/TiO_2	1.1×10^{-5}	Cho et al., 2010
	Singlet oxygen	Vis/C_{60}	1.1×10^{-5}	Cho et al., 2010
		Vis/erythrosine	5.0×10^{-6}	Ryberg et al., 2018
		Vis/RB	1.9×10^{-5}	This study

The inactivation of MS2 showed no lag phase (Fig. 3.5b), which may be attributable to the simpler structure of MS viral particles as compared to *E. coli* cells; MS2 has no barriers to shield from attacks by oxidants. The Chick-Watson model (Equation 3) was used to interpret the kinetics of MS2 inactivation. The inactivation rate of MS2 (the slope of the linear regression curve) was determined to be 1.1×10^5 log inactivation/(mg·min/L). The *Ct* value of $^1O_2$ required for 2 log inactivation of MS2 was 1.9×10^{-5} mg·min/L.

Table 1 summarizes the *Ct* values of oxidizing disinfectants required to achieve the 2-log inactivation of *E. coli* and MS2. The microbicidal efficacies of disinfectants as gauged from the *Ct* values (with lower *Ct* values indicating higher microbicidal efficacies) follow the order of chlorine ≈ chlorine dioxide < O_3 < $^1O_2$ < $^{\bullet}OH$, which is generally consistent with the order of oxidizing reactivity. The *Ct* value of $^1O_2$ for the inactivation of MS2 measured in this study (1.9×10^{-5} mg·min/L) was higher than those reported by previous studies (1.1×10^{-5} mg·min/L and 5.0×10^{-6} mg·min/L) (Cho et al., 2010, Ryberg et al., 2018) (also refer to Table 1); the different photosensitization systems used may have led to this discrepancy. A more drastic discrepancy in the disinfection kinetics has been reported for the inactivation of *E. coli* by $^{\bullet}OH$; the two *Ct* values reported in the literature were different by almost three orders of magnitude (8.0×10^{-6} mg·min/L for UV/TiO_2 and 4.5×10^{-9} mg·min/L for UV/H_2O_2, Table 1).

3.5. Environmental implication

Previous studies similar to this study did not investigate the inactivation effect of $^1O_2$ produced in a homogeneous system (Cho et al., 2010; Dahl et al., 1987; Dahl et al., 1989; Dahl et al., 1988; Bezman et al., 1978; Hotze et al., 2009; Müller- Breitkreutz et al.,1995; Schäfer et al., 2000; Ryberg et al., 2018; Jiménez-Hernández et al.,2006). It is very reasonable to say that most systems in which $^1O_2$ is produced have not confirmed the actual disinfection

performance of $^1O_2$, compared to that generated by irradiating visible light to a homogeneous system, especially the water quality in which natural organic substances exist. In addition, since most of the experimental systems are limited to viruses, the understanding of the inactivation kinetics of bacteria, which are relatively easy to proliferate and more infected cases are reported, is also relatively lacking. Based on the results of this study, it is expected to predict the inactivation effect of bacteria or viruses by naturally or artificially generated $^1O_2$ in the water system. In particular, since the (delayed) Chick-Watson model was applied, it can be said to be suitable for the most generalized disinfection performance evaluation method in a linear form, and it can show a high degree of understanding of self-healing by metabolism of bacteria.

Chapter 4. Cupric ion in combination with hydrogen peroxide and hydroxylamine applied to inactivation of different microorganisms

4.1. Results

4.1.1. Microbial inactivation by Cu(II)-based combined microbicides

The inactivation of four representative microorganisms, *E. coli* (a Gram-negative bacterium), *B. subtilis* (a Gram-positive bacterium), MS2 bacteriophage (a single-stranded RNA virus), and T4 bacteriophage (a double-stranded DNA virus), by Cu(II), Cu(II)/H_2O_2, Cu(II)/HA, Cu(II)/HA/H_2O_2 was examined (Fig 4.1); the degree of log inactivation increased linearly with the reaction time for all cases.

Cu(II) alone had minor or negligible microbicidal effects (< 1 log inactivation for bacteria (Fig. 4.1a and 1b) and < 0.5 log inactivation for MS2 and T4 (Fig. 4.1c and 1d) in 30 min). Cu(II)/H_2O_2 showed enhanced activity. In particular, the MS2 inactivation (1.15 log inactivation in 10 min (Fig. 4.1c)) was greater than the bacterial inactivation (0.95 log inactivation for *E. coli* (Fig. 4.1a) and 0.70 log inactivation for *B. subtilis* (Fig. 4.1b) in 15 min). Cu(II)/HA generally resulted in greater microbial inactivation than Cu(II)/H_2O_2; *E. coli* and *B. subtilis* were inactivated by 2.57 log and 1.45 log, respectively, in 15 min (Fig. 4.1a and 1b), and MS2 and T4 were by 1.50 log and 0.44 log in 30 min (similar to Cu(II)/H_2O_2) (Fig. 4.1c and 1d). The anoxic condition enhanced the inactivation of bacteria by Cu(II)/HA

(Fig. 4.1a and 1b), but it inhibited that of viruses (Fig. 4.1c and 1d). Cu(II)/HA/H_2O_2 generally led to the most microbial inactivation (except the anoxic Cu(II)/HA system for bacteria); *E. coli* and *B. subtilis* were inactivated by 4.67 log and 1.55 log (similar to Cu(II)/HA), respectively, in 15 min (Fig. 4.1a and 1b), and particularly the rates of MS2 and T4 inactivation was fast (3.83 log inactivation in 1 min (Fig. 4.1c) and 2.74 log inactivation in 5 min (Fig. 4.1d)).

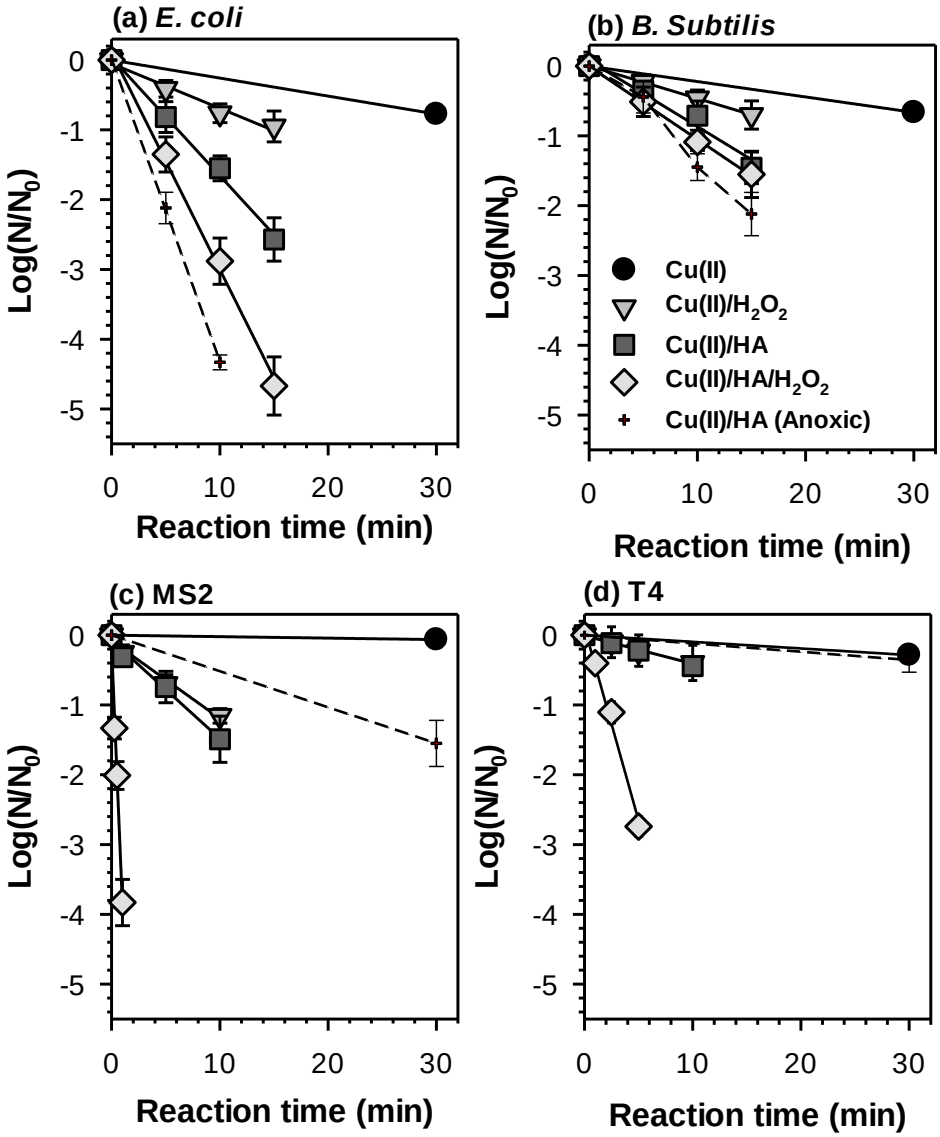

Fig. 4. 1. Inactivation of (a) *E. coli*, (b) *B. subtilis*, (c) MS2 bacteriophage, and (d) T4 bacteriophage by Cu(II), Cu(II)/H_2O_2, Cu(II)/HA, Cu(II)/HA (anoxic), and Cu(II)/HA/H_2O_2 ($[Cu(II)]_0$ = 5 μM, $[H_2O_2]_0$ = 10 μM, $[HA]_0$ = 10 μM, pH = 7.1).

The microbial inactivation by Cu(II), Cu(II)/H_2O_2, Cu(II)/HA, and Cu(II)/HA/H_2O_2 was tested for more bacterial and viral species (i.e., *V. harveyi*, *S. flexneri*, *S. typhimurium*, *P. aeruginosa*, *S. pneumoniae*, *S. Aureus*, T1 and T7 bacteriophages), and their inactivation rates (log

inactivation/min, calculated from the slopes of log inactivation curves) were presented (Fig. 4.2). The microbicidal activity (the rate of microbial inactivation) generally increased in the order of Cu(II) < Cu(II)/H_2O_2 < Cu(II)/HA < Cu(II)/HA/H_2O_2. The difference in microbicidal activity between Cu(II)/HA and Cu(II)/HA/H_2O_2 was relatively less for bacterial species (Fig. 4.2a–2h), compared to viral species (Fig. 4.2i–2l) which exhibited a very high susceptibility to Cu(II)/HA/H_2O_2.

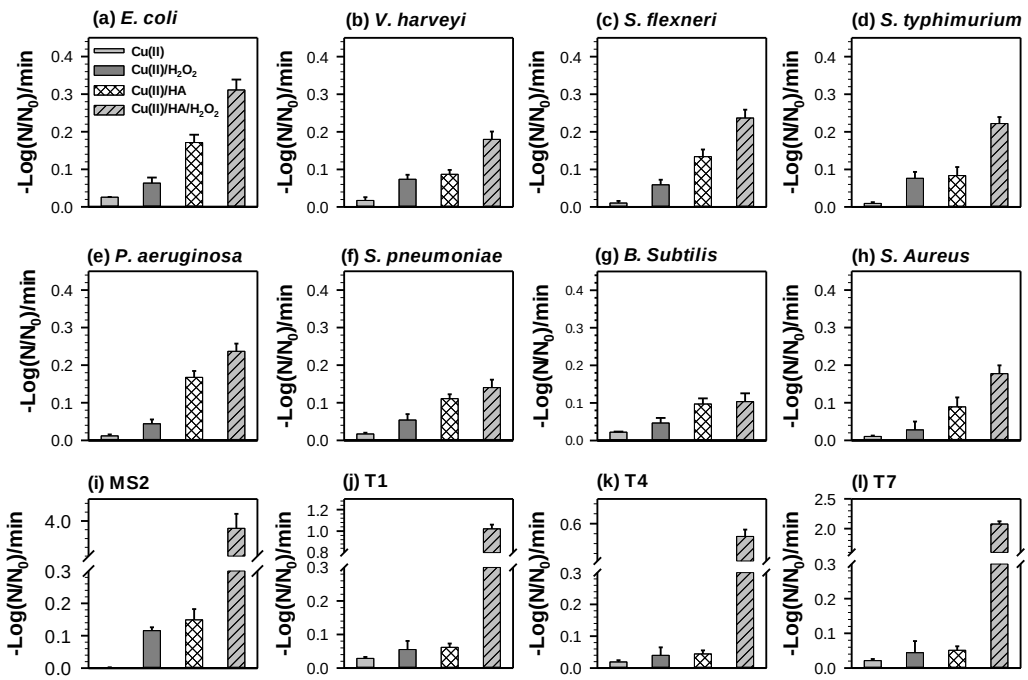

Fig. 4. 2. Inactivation rates of different bacterial and viral species by Cu(II), Cu(II)/H_2O_2, Cu(II)/HA, and Cu(II)/HA/H_2O_2 ($[Cu(II)]_0$ = 5 μM, $[H_2O_2]_0$ = 10 μM, $[HA]_0$ = 10 μM, pH = 7.1).

4.1.2. Microbicidal activity of Cu(II)/HA/H_2O_2 towards different microorganisms

The Cu(II)/HA/H_2O_2 system exhibited the greatest performance for the inactivation of all tested microorganisms, while its inactivation efficacy varies depending on the microbial species. In order to better compare the species-specific activity of Cu(II)/HA/H_2O_2, the inactivation kinetics of all tested microorganisms by Cu(II)/HA/H_2O_2 were depicted in single plots, the time-dependent log inactivation and the inactivation rate (Fig. 4.3). The results clearly show that the viral inactivation is much faster (by 6.25 folds in average) than the bacterial inactivation. Among the bacterial species, Gram-positive bacteria were more resistant to Cu(II)/HA/H_2O_2 than Gram-negative bacteria, and their inactivation rates were lower by 41% in average.

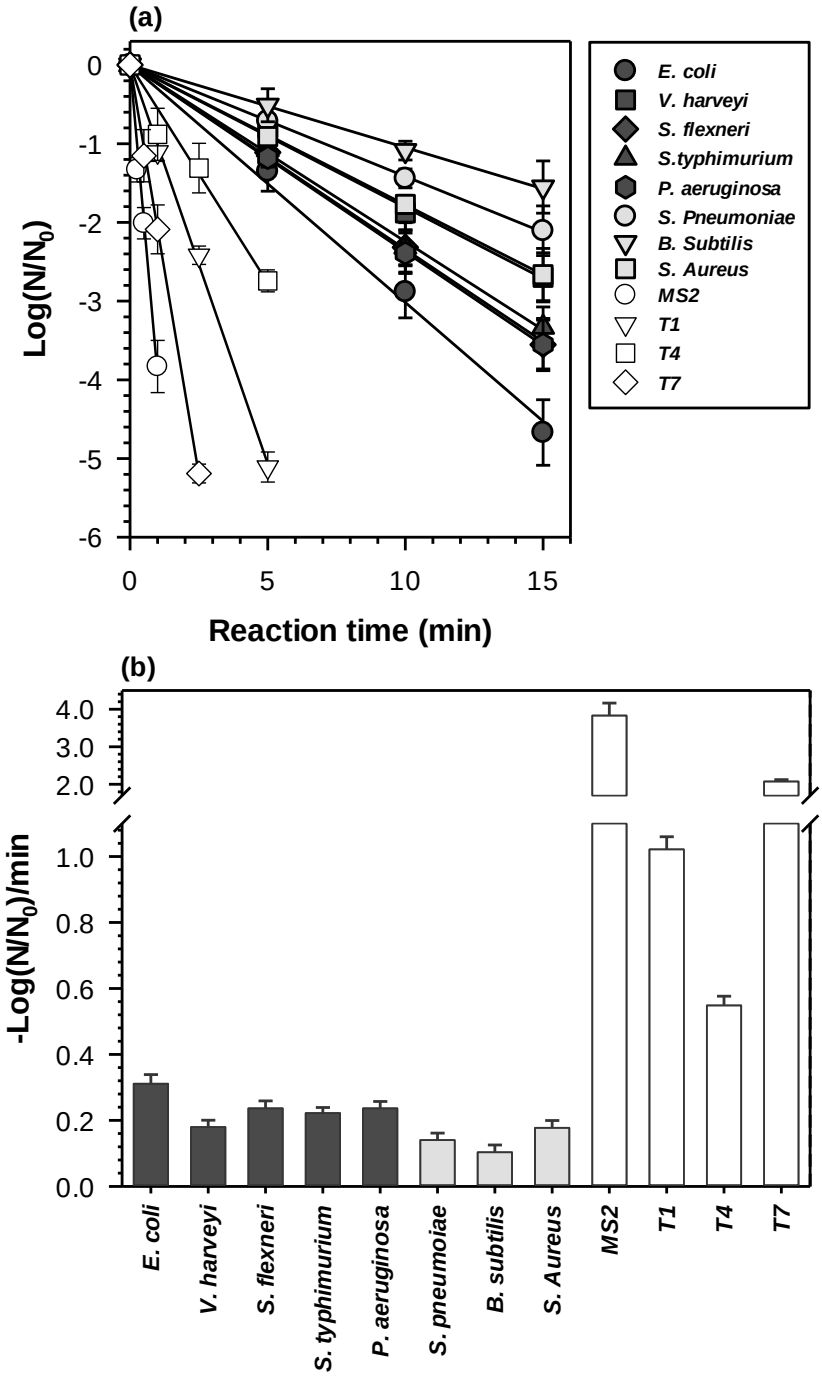

Fig. 4. 3. Inactivation of different bacterial and viral species by Cu(II)/HA/H_2O_2, (a) time-dependent inactivation curves and (b) inactivation rates ($[Cu(II)]_0$ = 5 μM, $[H_2O_2]_0$ = 10 μM, $[HA]_0$ = 10 μM, pH = 7.1).

4.1.3. Protein oxidation

The oxidation of proteins in microorganisms (mainly in viral capsids and bacterial cell membranes) was measured after treatment by Cu(II)/H_2O_2, Cu(II)/HA, and Cu(II)/HA/H_2O_2 (Fig 4.4). Different from the order of inactivation rate (i.e., Cu(II)/HA/H_2O_2 > Cu(II)/HA > Cu(II)/H_2O_2), the protein oxidation proceeded to a greater extent by Cu(II)/H_2O_2 than Cu(II)/HA (i.e., Cu/HA/H_2O_2 > Cu/H_2O_2 > Cu/HA). In general, viruses showed higher degrees of protein oxidation than bacteria; 25–42% of total proteins were oxidized by the Cu(II)/HA/H_2O_2 treatment. While Gram-positive bacteria showed lower inactivation rates by Cu(II)/HA/H_2O_2 than Gram-negative bacteria (Fig. 4.3), their degrees of protein oxidation were similar to or greater than those of Gram-negative bacteria (Fig. 4.4).

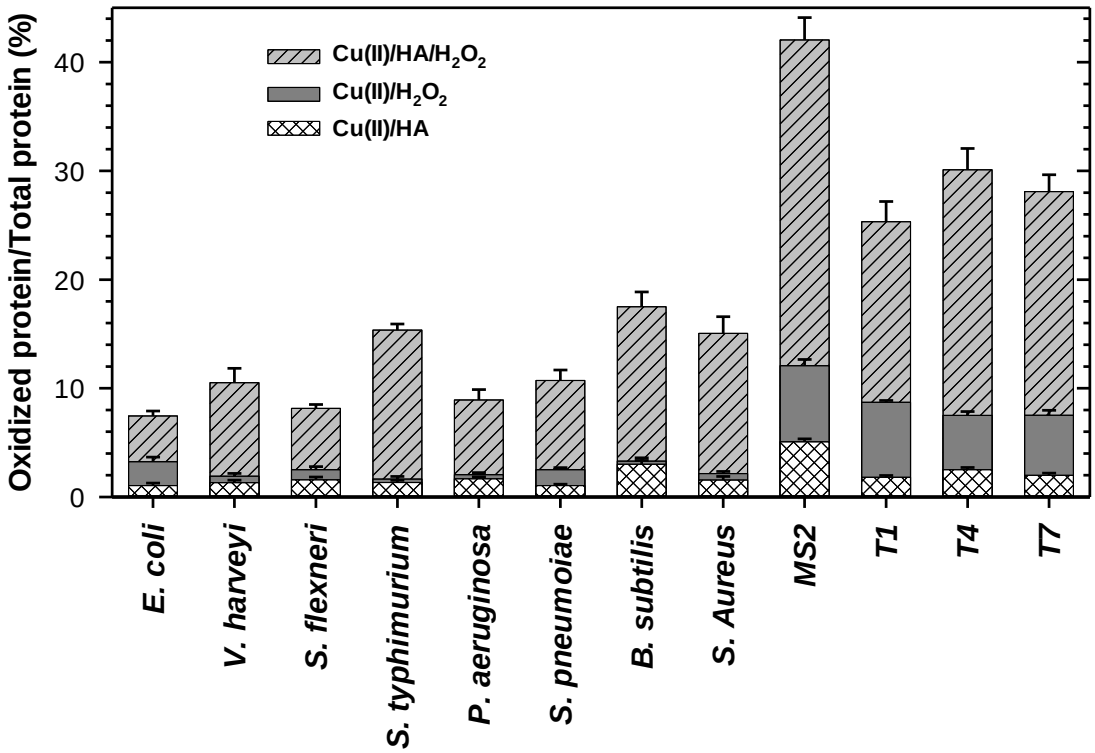

Fig. 4. 4. Protein oxidation of different bacterial and viral species after the treatment by Cu(II)/H_2O_2, Cu(II)/HA, and Cu(II)/HA/H_2O_2 ([Cu(II)]$_0$ = 5 μM, [H_2O_2]$_0$ = 10 μM, [HA]$_0$ = 10 μM, pH = 7.1, reaction time = 15 min (for bacteria), 10 min (for viruses)).

4.1.4. RNA (or DNA) damage

The damage of RNAs and DNAs in microorganisms was measured after the treatment by Cu(II)/H_2O_2, Cu(II)/HA, and Cu(II)/HA/H_2O_2 (Fig 4.5). In general, the RNA damage was greater with exogenous H_2O_2 (i.e., Cu/HA/H_2O_2 > Cu/H_2O_2 > Cu/HA), which is similar to the trend of protein oxidation. However, there were three exceptions (*S. pneumoiae* and *P. aeruginosa*) for which Cu/HA exerted more RNA damage. Gram-positive bacteria tended to show higher degrees of RNA damage than Gram-negative

bacteria. Meanwhile, the damage of viral RNAs was not much pronounced, contrary to the microbial inactivation rate and protein oxidation.

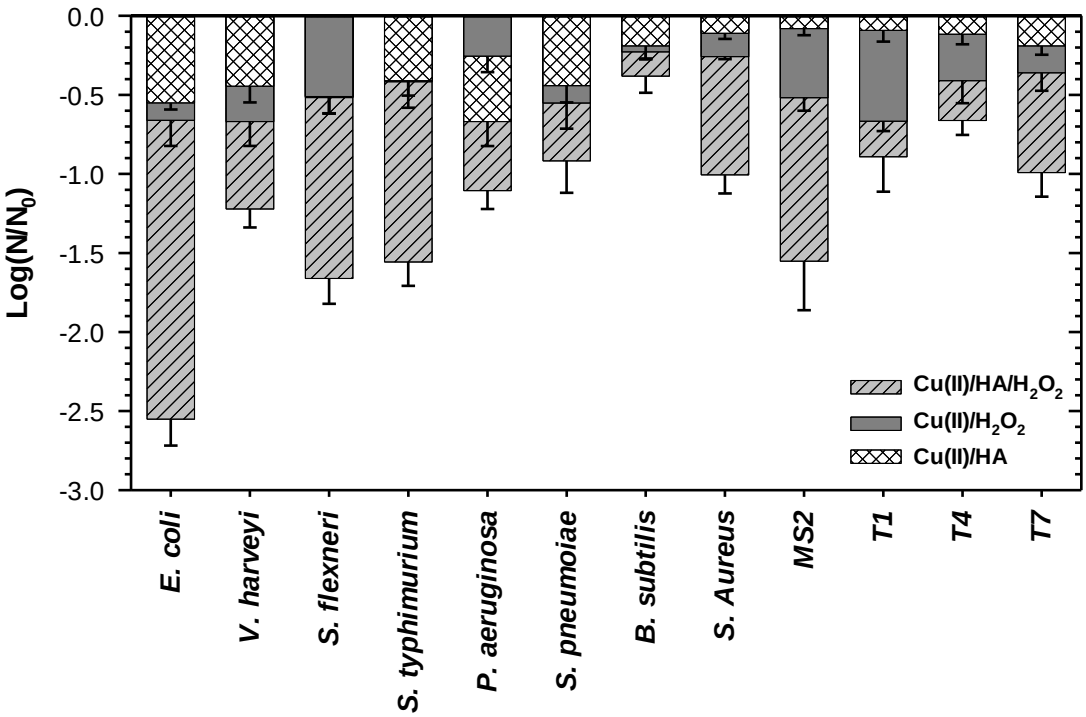

Fig. 4. 5. RNA (or DNA) damage of different bacterial and viral species after the treatment by Cu(II)/H_2O_2, Cu(II)/HA, and Cu(II)/HA/H_2O_2 ($[Cu(II)]_0$ = 5 μM, $[H_2O_2]_0$ = 10 μM, $[HA]_0$ = 10 μM, pH = 7.1, reaction time = 15 min (for bacteria), 10 min (for viruses)).

4.2. Discussion

4.2.1. Microbicidal effects of Cu(I) and Cu(III)

The microbial inactivation by Cu(II)/H_2O_2, Cu(II)/HA, and Cu(II)/HA/H_2O_2 is mainly explained by the microbicidal effects of Cu(I) and Cu(III) (Kim et al., 2015). It is believed that Cu(I) as a nonoxidative microbicide mainly leads to dysfunction of the protein biomolecules while

Cu(III) as a reactive oxidant causes oxidative damage to cellular components. Cu(I) and Cu(III) can be generated as intermediates by different redox reactions of Cu(II) with H_2O_2 and HA, and their steady-state concentrations will depend on the system (Cu(II)/H_2O_2, Cu(II)/HA, and Cu(II)/HA/H_2O_2) and conditions. Cu(II)/H_2O_2 produces Cu(I) and Cu(III) by the Fenton-like reactions (Reactions 4.1 and 2); Cu(III) rather than $^{\bullet}OH$ is believed to be generated as the major reactive oxidant (Lee et al., 2016).

$$Cu(II) + H_2O_2 \rightarrow Cu(I) + O_2^{\bullet-} + 2H^+ \quad (4.1)$$

$$Cu(I) + H_2O_2 \rightarrow Cu(II) + {}^{\bullet}OH + OH^- \text{ (minor)} \quad \text{or} \quad Cu(III) + 2OH^- \text{ (major)} \quad (4.2)$$

Cu(II)/HA also produces Cu(I) and Cu(III) by redox reactions involving HA and oxygen (Reactions 4.3–5). HA as a reducing agent converts Cu(II) into Cu(I) (Reaction 4.3), which subsequently reduces oxygen into H_2O_2 via a series of one-electron transfer reactions (Reaction 4.4 and 5). Then, the in situ-generated H_2O_2 is used to generate Cu(III) from Cu(I) (back to Reaction 2).

$$2NH_2OH \text{ (HA)} + 4Cu(II) \rightarrow N_2O + H_2O + 4Cu(I) + 4H^+ \quad (4.3)$$

$$Cu(I) + O_2 \rightarrow Cu(II) + O_2^{\bullet-} \quad (4.4)$$

$$Cu(I) + O_2^{\bullet-} + 2H^+ \rightarrow Cu(II) + H_2O_2 \quad (4.5)$$

Aside from the above reactions, Cu(II) can also be reduced by cellular components and intracellular $O_2^{\bullet-}$ (Park et al., 2012).

Cu(II)/H_2O_2 and Cu(II)/HA favor the production of Cu(III) and Cu(I), respectively, and Cu(II)/HA/H_2O_2 produces the greatest extent of Cu(III) by accelerating the H_2O_2-driven oxidation of Cu(I) into Cu(III) (Reaction 2) (Kim et al., 2015). The degrees of protein oxidation and RNA damage by the microbicidal treatments were in the order of Cu(II)/HA < Cu(II)/H_2O_2 < Cu(II)/HA/H_2O_2 (Figs. 4.4 and 5), indicating that Cu(III) is mainly responsible for the oxidative destruction of proteins and RNAs.

4.2.2. Bacterial inactivation

The inactivation of Gram-negative bacteria (*E. coli*, *V. harveyi*, *S. flexneri*, *S. typhimurium*, and *P. aeruginosa*) by Cu(II)/H_2O_2, Cu(II)/HA, and Cu(II)/HA/H_2O_2 is attributed to the simultaneous actions of Cu(I) and Cu(III). While the contributions of both Cu(I) and Cu(III) are important, the microbicidal susceptibility to Cu(I) appears to be higher, because Cu(II)/HA inactivates those bacteria to a greater extent than Cu(II)/H_2O_2 (Figs. 4.1 and 2). In particular, the anoxic Cu(II)/HA system (anticipated to generate more Cu(I)) causes the greatest degree of bacterial inactivation (Fig. 4.1a).

It is noteworthy that Gram-negative bacteria generally exhibit higher degrees of RNA damage compared to the other microbial species (Fig. 4.5), while the protein oxidation in these bacteria is not significant (Fig. 4.4). The relatively thin cell membranes (a thin single layer of peptidoglycan) of

Gram-negative bacteria can facilitate the penetration of microbicides into the cell, allowing more damage to their RNA (Breijyeh et al., 2020).

Gram-positive bacteria (*S. Pneumoiae*, *B. Subtilis* and *S. Aureus*) tended to show lower degrees of inactivation by Cu(II)-based combined microbicides (Fig. 4.2), particularly by Cu/HA/H_2O_2 (Fig. 4.3). The lower inactivation efficacy of Gram-positive bacteria is due to the thicker peptidoglycan layer in the cell membranes. Gram-positive bacteria usually showed a higher resistance to microbicides than Gram-negative bacteria. For example, according to literatures (Beuchat et al., 2005; Dow et al., 2006), *B. cereus*, a Gram-positive bacterium, was more resistant to chemical oxidants such as O_3 and chlorine by approximately 25 folds than *E. coli*. Gram-positive bacteria may have a higher resistance to Cu(III) (an oxidizing microbicide) than Cu(I), and this may result in a relatively smaller gap between the inactivation degree by Cu(II)/HA and Cu(II)/HA/H_2O_2 (Fig. 4.2f–2h). Cu(III) is believed to be mostly consumed by the cell membranes with the peptidoglycan layer, showing limited capability for cell penetration. This explanation is consistent with the observations that the protein oxidation by Cu(II)/HA/H_2O_2 in Gram-positive bacteria (largely by the oxidation of peptide chains of peptidoglycan) is slightly greater than that in Gram-negative bacteria (Fig. 4.4), while the RNA damage is much less (Fig. 4.5).

4.2.3. Viral inactivation

The distinctly fast inactivation of viruses by Cu/HA/H_2O_2 (Figs. 4.1–3) indicates that Cu(III) is a highly sensitive virucide. Cu(I) appears to be a much weaker virucide than Cu(III), which is evidenced by the suppression of viral inactivation by Cu(II)/HA under anoxic conditions (anticipated to generate little Cu(III)) (Figs. 4.1c and 1d). The degrees of protein oxidation for viruses were higher than those for bacteria (Fig. 4.4), whereas the viral RNA damage was not prominent (Fig. 4.5), which indicates that the oxidative damage of the protein capsid by Cu(III) is critical to the viral inactivation. Among the tested viruses, MS2 showed higher inactivation rates by Cu/HA/H_2O_2 than T series bacteriophages (T1, T4, and T7) (Fig. 4.3), which is consistent with higher degrees of protein oxidation and RNA damage for MS2 (Figs. 4.4 and 5). T series bacteriophages are larger and more complex than MS2 (Leiman et al., 2003; Kuzmanovic et al., 2006), and possibly are more resistant to the attack of Cu(III).

4.3. Environmental implication

Due to the recent outbreak of various infectious diseases and their counteraction, research on inactivation of microorganisms by various disinfectants is continuously increasing. In particular, studies on the inactivation of microorganisms using the toxicity of metals, for example, copper or silver, have been actively conducted recently. On the other hand,

in the case of silver, it is not suitable for disinfection due to its excessively high toxicity and its relatively high price because it is a precious metal. For this reason, research on copper-based disinfection systems has recently been actively performed (Kim et al., 2015; Lee et al., 2017, Beswick et al., 1976; Chen et al., 2013; Kirakosyan et al., 2008; Park et al., 2012). Since copper is a transition metal, it is characterized by being able to have various valences, and divalent is known as the most stable form in nature.

However, toxicity (inhibition of metabolic rate) of Cu(I) due to characteristics with amino acid monomers and very high binding energy and high oxidizing potential of Cu(III) would show different disinfection properties, but the identification of these was very insufficient. Through this study, the selectivity of each disinfectant was confirmed through the application of Cu(I) and Cu(III) to the inactivation of various microorganisms, which is expected to contribute highly to the applicability evaluation of the disinfectant. In addition, through the results of investigating the inactivation mechanism, the extent to which damage to each organelle contributes to the inactivation of microorganisms was identified, which is expected to serve as basic data for future studies.

Chapter 5. Inactivation kinetics and mechanisms of corona and adeno virus by conventional disinfectant in aqueous media

5.1. Viral inactivation by conventional disinfectants.

The inactivation of AdV and CoV by 3 different conventional disinfectant under aqueous condition was examined (Fig. 5.1.); The degree of log-scale viral inactivation linearly correlated with reaction time for all cases. On the other hands, in the case of free chlorine and H_2O_2 the decomposition of oxidants was negligible whereas O_3 was completely decomposed within 20 sec (the insets of Fig. 5.1).

O_3 showed the superior inactivation efficacy with 3.3 log inactivation for AdV and 2.8 log inactivation for CoV within 15 sec (Fig. 5.1a), whereas free chlorine showed 2.0 log for AdV and 4.2 log for CoV within 10 min (Fig. 5.1b), respectively. H_2O_2 had the lowest disinfection efficacy with 3.0 log for AdV and 0.9 log for CoV within 15 min (Fig. 5.1c). However, O_3 is decomposed rapidly to be completely decomposed within 20 seconds (the insets of Fig. 5.1a), there is a possibility for showed relatively low disinfection efficacy when comparing the *Ct* (concentration-time product) values of oxidants. Since the lag phase and shoulder were not observed, the *Ct* value was obtained by applying the Chick-Watson model in this study.

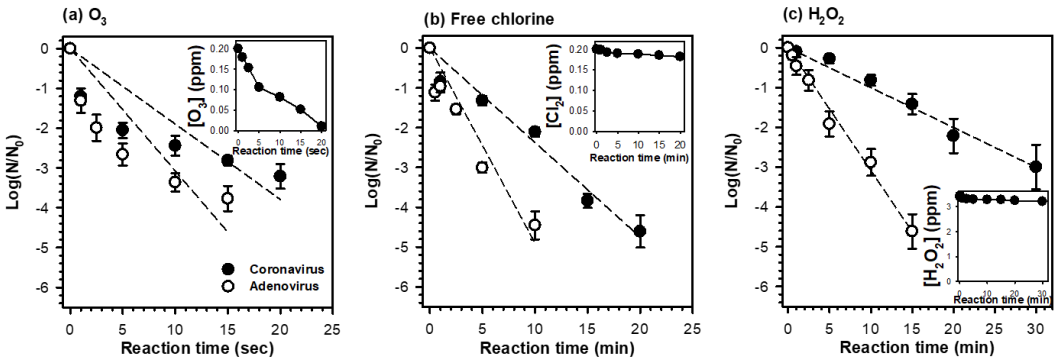

Fig. 5. 1. Inactivation of AdV and CoV by O_3 (a), free chlorine (b) and H_2O_2 (c) (insets ; decomposition of oxidants)

($[AdV]_0 = [CoV]_0 = 10^7$ PFU/mL; $[O_3]_0$ = [Free chlorine]$_0$ = 0.2 ppm; $[H_2O_2]_0$ = 3.4 ppm; [tris buffer] = 30 mM; pH = 7.3; Temperature = 20°C).

The viral inactivation efficacy as function of oxidant concentration and reaction time was determined (Fig. 5.2). The *Ct* of oxidants required for 2 log inactivation of CoV with single oxidant concentration (0.2 ppm for O_3 and free chlorine, 3.4 ppm for H_2O_2) were founded to be 0.01023 (O_3), 1.391 (free chlorine) and 64.935 (H_2O_2) mg·min/L, respectively. When *Ct* required for 2 log inactivation of AdV were 0.00723 (O_3), 0.729 (free chlorine) and 21.008 (H_2O_2) mg·min/L. According to *Ct*, although the residual O_3 concentration is continuously decreased by O_3 decomposition, it can be determined that O_3 has the strongest virucidal potential. On the other hand, inactivation of AdV for all oxidants showed higher efficiency than inactivation of CoV, which can be inferred from the morphological factors such as the presence of surface covering envelope and size distribution (90 - 100 nm for AdV and 120 – 200 nm for CoV). For a same reason, the difference in *Ct* between H_2O_2, a less effective oxidants, and O_3, an

effective oxidants, in AdV showed 20-folds, whereas in CoV it showed 60-folds.

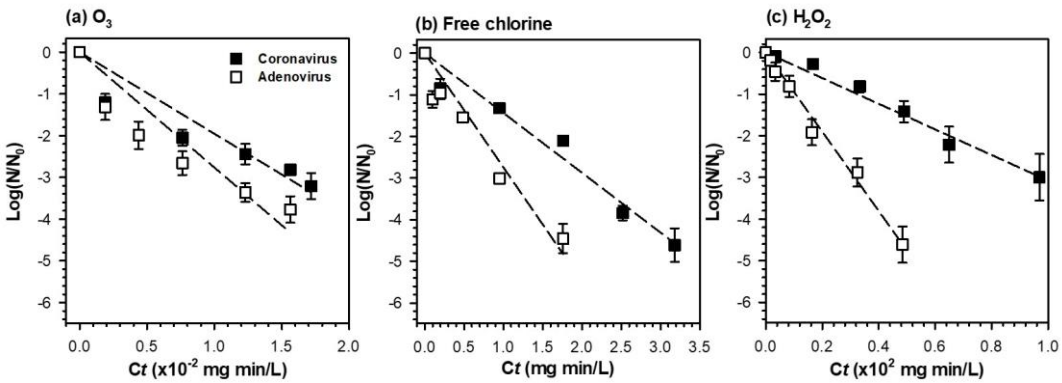

Fig. 5. 2. *Ct* values for AdV and CoV inactivation by O_3 (a), free chlorine (b) and H_2O_2 (c) ($[AdV]_0 = [CoV]_0 = 10^7$ PFU/mL; $[O_3]_0$ = [Free chlorine]$_0$ = 0.2 ppm; $[H_2O_2]_0$ = 3.4 ppm; [tris buffer] = 30 mM; pH = 7.3; Temperature = 20°C).

5.2. Changes of viral inactivation as function of pH

The *Ct* plot of AdV and CoV inactivation by free chlorine under various free concentrations was examined at three pH values ranging from 6.5 to 8.6 (Fig. 5.3). The inactivation efficacy of CoV was significantly higher at pH 8.6 than at pH 6.5 and 7.3, when inactivation of AdV showed opposite trends. The disinfection efficacy eventually changes due to one of the following reasons: species change of the oxidants or changes in the state of the virus as function of pH. According to previous studies, free chlorine species change into HOCl and OCl^- depending on the pH, and it is generally known that HOCl has a higher disinfection ability than OCl^- at the same concentration. Therefore, the CoV has proven, which is accelerated in the

opposite direction to the species change of the oxidants, has a change in the state of the virus according to the pH.

The correlation between the *Ct* plot and pH according to the type of virus at various oxidant concentrations was shown (Fig. 5.3). In the case of O_3, the higher pH, the more stable it was, so for both viruses showed the higher the disinfection ability when pH increased. However, in the case of CoV, it showed a larger increase rate compared to the 1.6-fold increase rate of AdV with an improvement in disinfection efficacy of 2-fold. The *Ct* of H_2O_2 required for 2 log inactivation of CoV were founded to be 51.948 (pH 6.5), 60.606 (pH 7.3) and 22.753 (pH 8.6) mg·min/L, respectively. When *Ct* required for 2 log inactivation of AdV were 21.322 (pH 6.5), 47.281 (pH 7.3) and 58.309 (pH 8.6) mg·min/L. The pKa of H_2O_2 is 11.75, which is significantly different from the experimental condition, but a 1.2-fold decrease in disinfection efficacy was observed in AdV according to the increase in pH.

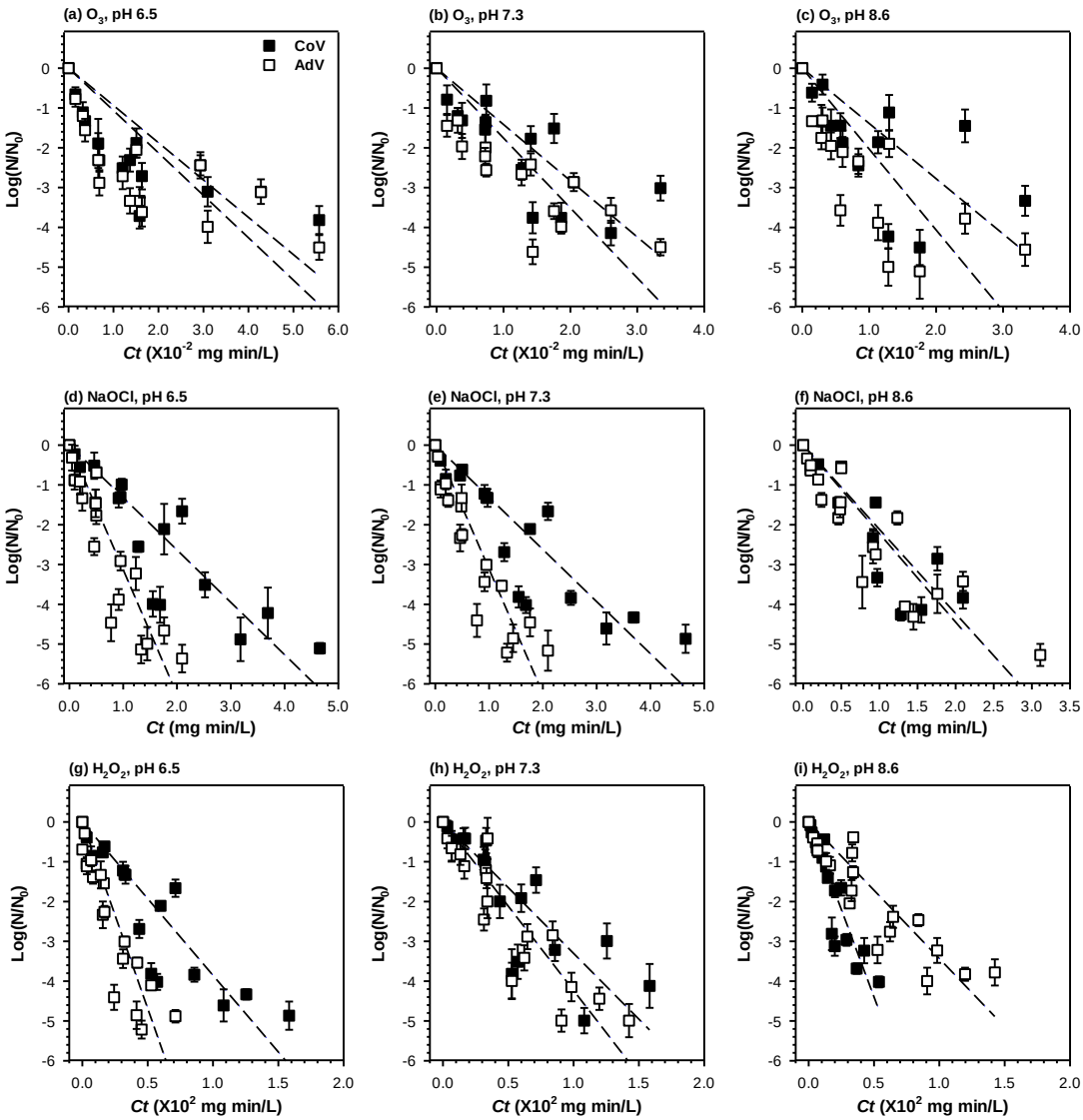

Fig. 5. 3. Differences of *Ct* values for AdV and CoV inactivation by oxidant at various pH; free chlorine (a-c), O_3 (d-f) and H_2O_2 (g-i).

($[AdV]_0 = [CoV]_0 = 10^7$ PFU/mL; $[O_3]_0$ = [Free chlorine]$_0$ = 0.2 ppm; $[H_2O_2]_0$ = 3.4 ppm; [tris buffer] = 30 mM; Temperature = 20°C).

Table5.1. CT values for achieving 2 log microbial inactivation by chlorine

Species	CT value (mg·min/L)	Experimental condition	Reference
E. Coli	0.17	Phosphate buffer, pH 7.1, 20 ℃	(a)
Lactococcus sp.	5.0	Saline buffer, pH 7.1, 20 ℃	(b)
B. Subtilis	130	Phosphate buffer, pH 7.1, 20 ℃	(c)
L. Pneumophila	0.135	Natural water, pH 7.3, 4 ℃	(d)
S. Aureus	2800	Phosphate buffer, pH 7.1, 20 ℃	(e)
E. tarda	0.0746	Phosphate buffer, pH 8.2, 4 ℃	(f)
Rotavirus	0.4	w/o, pH 7.0, 20 ℃	(g)
Murine norovirus	0.036	w/o buffer, pH 7.2, 5 ℃	(h)
Hepatitis A	N.A. (16 for 4 log inactivation)	w/o buffer, pH 6~9, 5~15 ℃	(i)
MS2 coliphage	2.06	w/o buffer, pH 7, 18~22 ℃	(j)
Corona virus(NL63)	0.67 (pH 8.6)~1.52 (pH 6.5)	Tris buffer, pH 6.5~8.6, 20 ℃	This study
Adeno virus	0.087	w/o buffer buffer, pH 6~8, 5 ℃	(h)
	0.945	Tris buffer, pH 6.5~8.6, 20 ℃	This study

(a) Cho et al., 2010 (b) Tanaka et al., 2013 (c) Cho et al., 2006 (d) Landeen et al., 1989 (e) Kim et al., 2008 (f) Cho et al., in preparation (g) Rose et al., 2005
(h) Rachmadi et al., 2020 (i) USEPA Protocol, 1991 (j) Shang et al., 2007

Table. 5.2 CT values for achieving 2 log microbial inactivation by ozone

Species	CT value (mg·min/L)	Experimental condition	Reference
E. Coli	0.004	Phosphate buffer, pH 7.1, 4 ℃	(a)
P. Aeruginosa	0.052	w/o buffer, pH 7.2, 25 ℃	(b)
B. Subtilis	3.7	w/o buffer, pH 6.0, 4 ℃	(c)
S. Typhi	0.051	w/o buffer, pH 7.2, 25 ℃	(b)
V. Harveyi	0.00279	Phosphate buffer, pH 6.5~8.2, 4 ℃	(d)
E. tarda	0.00280	Phosphate buffer, pH 6.5~8.2, 4 ℃	(d)
Murine norovirus	0.72	Phosphate buffer, pH 7, 20 ℃	(e)
Rotavirus	0.026	Natural water, 18 ℃	(f)
MS2 coliphage	0.17	Phosphate buffer, pH 7.0, 20 ℃	(g)
PhiX174	0.010	Saline buffer, pH 3.0, 22 ℃	(h)
Echovirus	0.052	Saline buffer, pH 3.0, 22 ℃	(h)
Corona virus(NL63)	0.0112(pH 8.6)~0.0187(pH6.5)	Tris buffer, pH 6.5~8.6, 20 ℃	This study
Adeno virus	0.0131	Tris buffer, pH 6.5~8.6, 20 ℃	This study

(a) Hunt et al., 1997 (b) Lezcano et al., 1999 (c) Cho et al., 2005 (d) Kim et al., in preparation (e) (f) Langlais et al., 1991 (g) Cho et al., 2008 (h) Wolf et al., 2018
(i) Shang et al., 2007

5.3. Responsibility of viral inactivation

The damage of gene and oxidation of protein and lipid was measured after the treatment by O_3, free chlorine and H_2O_2. The responsibility of microbial inactivation was expressed by normalizing the relative values of oxidized or damaged genes, proteins, and lipids with initial values and dividing by the inactivation rate of microorganisms (Fig. 5.4-6). The inactivation responsibility not identified by the three inactivation mechanisms was expressed as an unknown contribution, for example, a synergistic effect, and the sum of the four factors was set to 100%. The surrogate Gram-positive bacteria (*B. subtilis*), Gram-negative bacteria (*E. coli*), and bacteriophage (MS2) were added one by one for a more sophisticated relative comparison. The *Ct* values of bacteria and viruses for achieving 2 log inactivation are presented in Tables 5.1 and 2. In O_3 treatment, the decomposition of lipids was promoted as the pH of both pathogenic viruses increased, and it was elucidated that the most important inactivation mechanism was ozonation. In addition, it has the lowest proportion of unknown compared to the other two species of oxidants, which means that the dominant inactivation mechanism is clearly damaging on viruses. In the case of CoV, it was shown that the ratio of protein degradation continued to decrease as the pH increased. However, this is due to the increasing degree of inactivation of the CoV, and the actual amount of protein degradation did not increase.

Inactivation of AdV by free chlorine was contributed by each of the four inactivation mechanisms in almost equal proportions regardless of pH. On the other hand, in the case of CoV, it was confirmed that the degradation of lipids was continuously increased while the degradation of proteins was continuously decreased as the pH was increased. In the case of *E. coli*, *B. subtilis*, and MS2, there was no significant correlation, but at pH 7.3, the degradation of lipids in *E. coli*, proteins in *B. subtilis*, and genes in the case of MS2 was significantly increased.

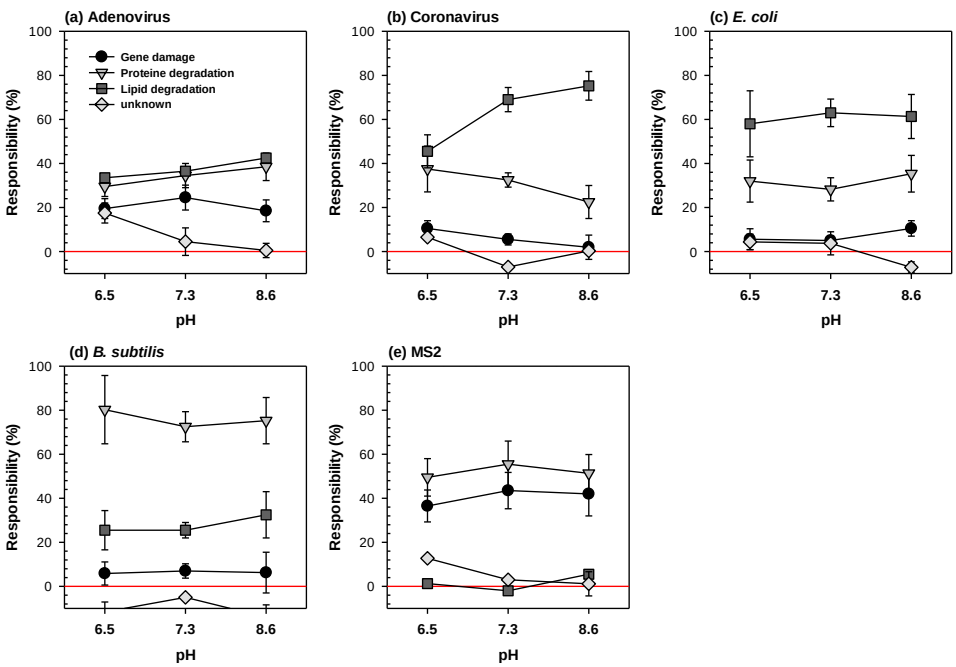

Fig. 5. 4. Changes of responsibility for microbial inactivation by O_3 as function of pH ($[MO]_0$ = 10^7 CFU or PFU/mL; $[O_3]_0$ = 0.2 ppm; [tris buffer] = 30 mM; Temperature = 20°C).

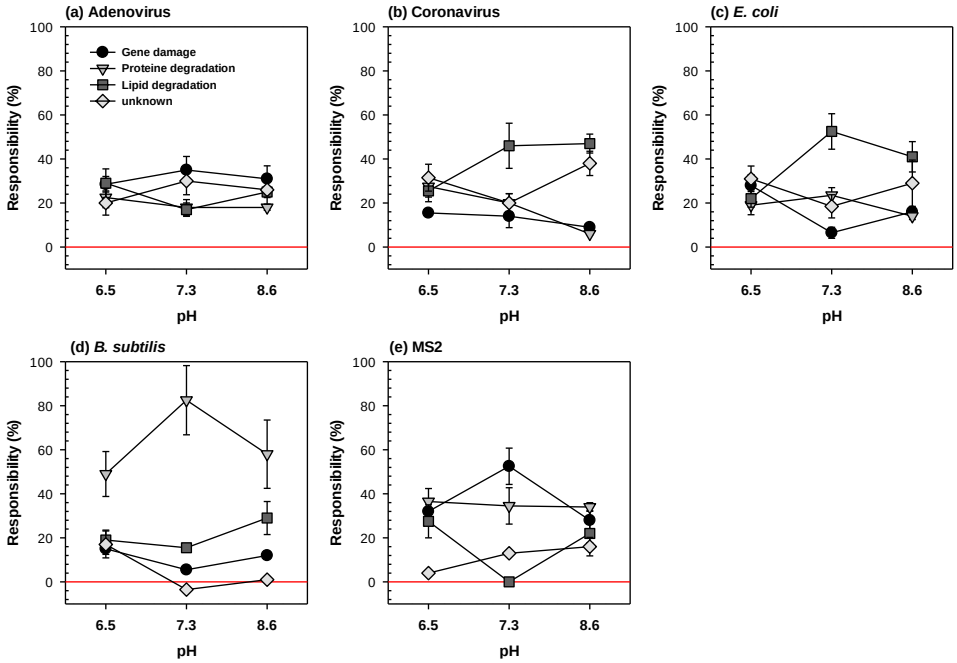

Fig. 5. 5. Changes of responsibility for microbial inactivation by Free chlorine as function of pH

([MO]$_0$ = 10^7 CFU or PFU/mL; [Free chlorine]$_0$ = 0.2 ppm; [tris buffer] = 30 mM; Temperature = 20°C).

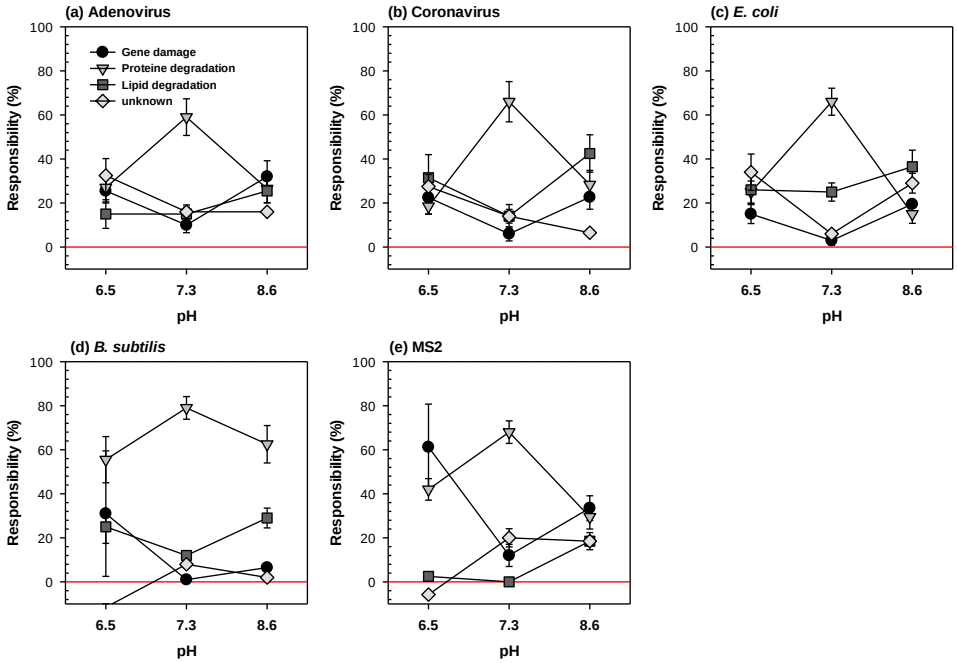

Fig. 5. 6. Changes of responsibility for microbial inactivation by H_2O_2 as function of pH ($[MO]_0 = 10^7$ CFU or PFU/mL; $[H_2O_2]_0 = 3.4$ ppm; [tris buffer] = 30 mM; Temperature = 20°C).

Upon inactivation by H_2O_2, the highest protein degradation was observed at pH 7.3 for both AdV and CoV. A similar trend was observed for all other microorganisms. On the other hand, gene damage did not show a significant correlation, and the decomposition of lipids was accelerated in a constant trend as the pH increased. The ratio of unknown varied according to the increase or decrease of other inactivation mechanisms, and a change in a certain trend could not be shown. As it is known that H_2O_2 does not change species or stability according to pH in this experimental condition, changes in the state of the components of microorganisms have an effect. Therefore, it seems most likely that the increase in the inactivation degree of

the corona virus according to the increase in pH is due to the accelerated decomposition of the lipids contained in the envelope and the spike, and the infectivity is greatly reduced.

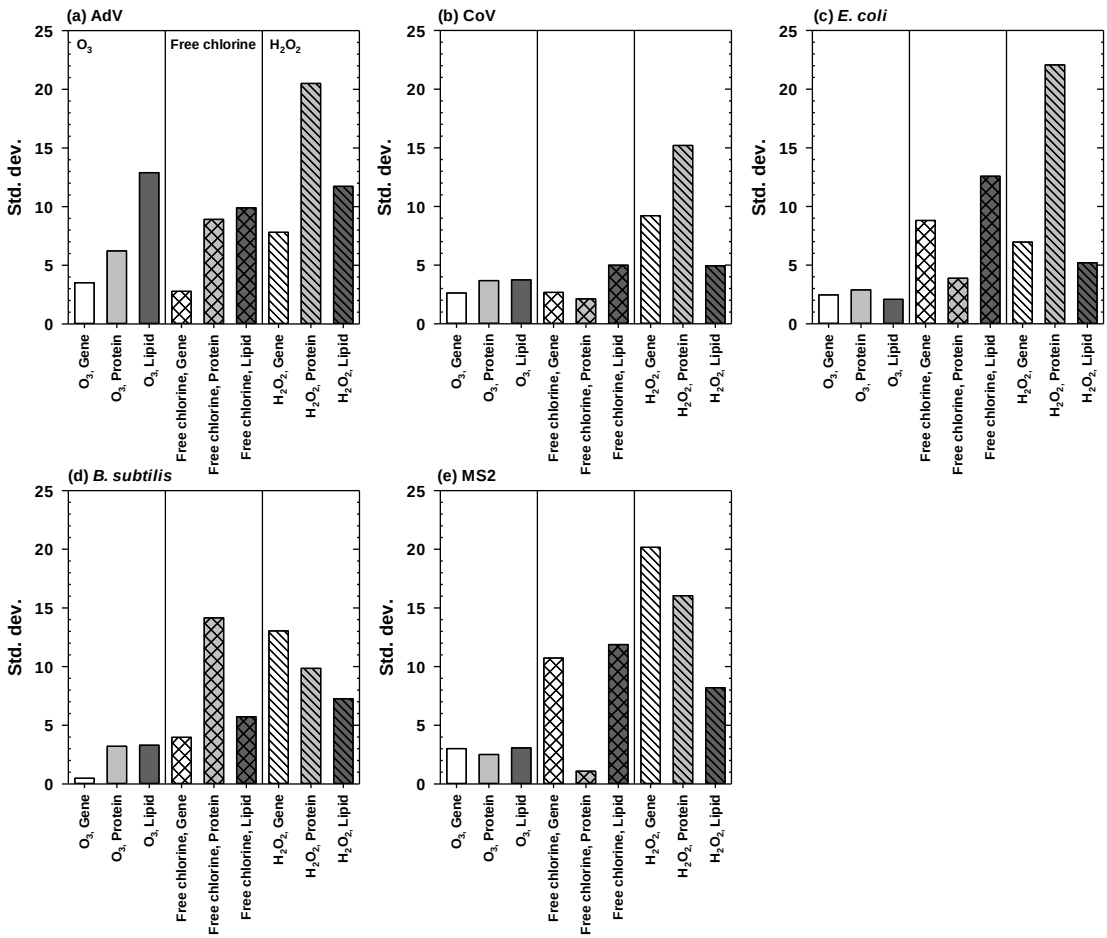

Fig. 5. 7. Standard deviation of inactivation mechanisms for microbial inactivation by oxidant as function of pH

([MO]$_0$ = 10^7 CFU or PFU/mL; [O_3]$_0$ = [Free chlorine]$_0$ = 0.2 ppm; [H_2O_2]$_0$ = 3.4 ppm; [tris buffer] = 30 mM; Temperature = 20°C).

All other variables need to be controlled in order to establish that the contribution to the change in microbial inactivation by pH is entirely due to the correlation between microbial functional groups and pH. In this study, the exposure amount or species change of oxidants, which can be changed by pH, was continuously monitored, and experiments were conducted with metal ions or organic contaminants completely removed to confirm possible mechanism changes. The effect of the pH change on the microbial inactivation mechanism was confirmed through the dispersity of each microbial inactivation mechanism according to the change in pH (Fig. 5.7.). Free chlorine or O_3 undergoes changes such as a species change or its own decomposition rate becoming faster in the pH of the experimental area, but H_2O_2 does not undergo such a change in the corresponding pH area. Therefore, since all variables are controlled, the difference in contribution to microbial inactivation by H_2O_2 is sufficient grounds to determine that it is solely due to the change in the functional group of microorganisms. The result of the acceleration of the degree of protein degradation according to the change in pH, the change in responsibility, and the insignificant difference in the absolute amount of degradation can confirm that the change in pH accelerates the degradation of other components. From this result, protein is not dependent on pH unlike other components.

5.3. Environmental implication

In this study, the application of water treatment technology was presented as a response technology that can respond to the outbreak of COVID-19, which has recently become a problem. SARS-CoV-2, the causative agent of COVID-19, is characterized by high infectivity in the air, and infectivity in water systems has not generally been proven. However, it is necessary to consider the fact that the medium of all contact is water, and the possibility of transmission by droplets (by coughing, etc.).

Among water treatment technologies, in the case of disinfection technology using an oxidant as a disinfectant, the oxidizing power can vary greatly depending on the pH of the water system, and in general, free chlorine shows high activity in a low pH region and O3 in a high pH region. However, in the results of this study, it was confirmed that the higher the pH, the higher the activity was consistently. In order to confirm this, a study on the disinfection mechanism was performed, and it was confirmed that the decomposition of lipids accelerated as the pH increased. Therefore, it was confirmed that enveloped viruses such as CoV or viruses with high lipid content show high inactivation efficiency at high pH, thick capsid at low pH, and generally at neutral pH.

Chapter 6. Conclusion

6.1. Summary

For the photosensitized system (RB/vis), no significant microbial inactivation was observed in the absence of oxygen or in the presence of an excess of $^1O_2$ scavenger, indicating that $^1O_2$ is a responsible disinfectant. The concentration of RB had a slight effect on microbial inactivation. Increasing the incident light intensity increased the inactivation efficiency of *E. coli* and MS2 almost linearly. Microbial inactivation was found to correlate with Ct. An early lag phase can be observed in the inactivation curve of *E. coli*. A (delayed) Chick-Watson model was applied to the *Ct* plot.

The Cu(II)-based complex fungicides (Cu(II)/H_2O_2, Cu(II)/HA and Cu(II)/HA/H_2O_2 systems) can effectively inactivate 12 species of bacteria and viruses in water. Cu/HA/H_2O_2 used in the experiment showed the highest inactivation efficiency against all target microorganisms. The bactericidal effect of Cu(II)/H_2O_2, Cu(II)/HA, Cu(II)/HA/H_2O_2 is mainly explained by the role of Cu(I) and Cu(III) produced as intermediates by redox reaction. became It has been found that Cu(I), a non-oxidizing disinfectant, is more effective at inactivating bacteria than viruses, whereas Cu(III), a reactive oxidizing agent, is sensitive to inactivation of viruses. In general, Gram-positive bacteria with thick peptidoglycan walls were more resistant to fungicides than Gram-negative bacteria.

The inactivation kinetics and mechanisms of CoV and AdV in

aquatic system using conventional disinfectants. It was found that parameters such as changes in pH and concentration of oxidants cause significant changes in virus inactivation kinetics and its mechanisms. In the inactivation of CoV at high pH, the degradation of lipids was responsible for the inactivation of microorganisms. In AdV, it was determined that all inactivation mechanism had equally contributed. By continuously measurement of the oxidant concentration over the time intervals, it was found that viral inactivation linearly correlated with *Ct*.

6.2. Conclusion & implications

The results of this study demonstrated that the dominant microbial inactivation mechanism can be changed depending on the microbial species, the type of oxidant, and the experimental conditions, and the type and concentration of the optimal oxidant for each microbial species can be experimentally confirmed. In inactivation of microorganisms, it is reasonable to design optimally by not only the oxidation potential of the oxidant but also various factors such as the composition of microorganisms and pH. Experimentally, in the case of Gram-positive bacteria, a toxic disinfectant such as Cu(I) may be advantageous, and Gram-negative bacteria also show high inactivation efficiency of oxidants. If the virus has an envelope, the inactivation efficiency can be greatly reduced, so caution is required.

Most of the previous studies focused on simple microbial inactivation and did not prioritize adding quantitative and qualitative interpretations of microbial inactivation. In the inactivation of $^1O_2$, its own disinfecting ability or the possibility of inactivating viruses and bacteria was suggested, but there is virtually no study to quantitatively evaluate the contribution of pure $^1O_2$ to the inactivation of microorganisms in a homogeneous system (Cho et al., 2010; Dahl et al., 1987; Dahl et al., 1989; Dahl et al., 1988; Bezman et al., 1978; Hotze et al., 2009; Müller-Breitkreutz et al.,1995; Schäfer et al., 2000; Ryberg et al., 2018; Jiménez-Hernández et al.,2006). In the study conducted in this dissertation, in order to quantitatively evaluate the inactivation of viruses or bacteria by pure $^1O_2$ generated in a homogeneous system, the inactivation by excited dyes was eliminated by controlling the experimental variables. These results provide a complete understanding of the utility of $^1O_2$ for inactivation of microorganisms in future studies.

Studies on the specificity of each copper species in the inactivation of microorganisms by copper-based disinfectants have already been conducted through previous studies (Kim et al., 2015; Lee et al., 2017, Beswick et al., 1976; Chen et al., 2013; Kirakosyan et al., 2008; Park et al., 2012). However, it was very insufficient to fully understand the inactivation of microorganisms using copper-based disinfectants, such as not investigating the disinfection ability for a sufficiently large number of microorganisms or qualitatively explaining the mechanism. Therefore, in

this study, inactivation was confirmed for 12 types of microorganisms, including Gram-positive bacteria, negative bacteria, and viruses with various structures, and a qualitative analysis was performed on the inactivation mechanism. As a result of the study, the inactivation of microorganisms by copper-based disinfectants was confirmed that Cu(III) was a virus-specific disinfectant, and it was confirmed that most of them were inactivated by oxidation of proteins. Cu(III) is a metal ion with high oxidizing power, and it is thought to inactivate microorganisms by oxidizing protein components of membranes or capsids of microorganisms. Based on this result, it seems very easy to apply Cu(III) to inactivate microorganisms with high protein content or to inactivate viruses. Since only copper ions at a lower concentration than the water quality standard are used in the water system, active additional research is needed.

Quantitative analysis of the inactivation of two infectious virus species, CoV and AdV, in aqueous system was completely absent. Although the possibility of transmission of respiratory viruses through water systems has been suggested through several literatures, most researchers have dismissed the possibility as very low and ignored the need for sterilization through water treatment. However, such a study must be carried out because the virus transmitted through the respiratory system is always included in the water droplet, and even if the possibility of transmission of the virus through the water system is low, the ripple effect is likely to be very high if it occurs. Through this study, the inactivation of viruses in the water system

according to the type of disinfectant was quantitatively analyzed, and the inactivation mechanism contributing to the inactivation of the virus was qualitatively analyzed. As a result of the study, it was confirmed that the degree of inactivation of the virus in the water system varies depending on the pH and the type and concentration of the oxidizing agent, and it was confirmed that this can be quantitatively evaluated. By qualitatively analyzing the contribution of virus inactivation, it was confirmed that the higher the pH, the faster the virus inactivation, assuming that all other conditions are the same. Based on this result, when inactivating viruses with high lipid content in the future, higher inactivation efficiency can be expected at higher pH conditions together with the type and concentration of the oxidizing agent. In addition, a synergistic effect can be expected when it is a more stable oxidant at high pH or when self-decomposition is accelerated to produce a stronger oxidant.

Reference

Amrullah, A., Paksung, N., Matsumura, Y., 2019. Cell structure destruction and its kinetics during hydrothermal treatment of sewage sludge. Korean J. Chem. Eng. 36(3), 433-438.

APHA, 2005. Standard methods for the examination of water and wastewater, 21st ed., APHA: Washington, DC, USA.

Bednarski, D. M., Lantz, E. E., Bobst, C. E., Eisenhut, A. R., Eyles, S. J., Fey, J. P. 2020. Sterilization of epidermal growth factor with supercritical carbon dioxide and peracetic acid; analysis of changes at the amino acid and protein level. Biochimica et Biophysica Acta (BBA) - Proteins and Proteomics, 1868(2), 140334.

Beswick, P. H., Hall, G. H., Hook, A. J., Little, K., McBrien, D. C. H., Lott, K. A. K., 1976. Copper toxicity: Evidence for the conversion of cupric to cuprous copper in vivo under anaerobic conditions. Chem. Biol. Interact. 14, 347-356.

Beuchat, L. R., Pettigrew, C. A., Tremblay, M. E., Roselle, B. J., Scouten, A. J., 2004. Lethality of chlorine, chlorine dioxide, and a commercial fruit and vegetable sanitizer to vegetative cells and spores of Bacillus cereus and spores of Bacillus thuringiensis. J. Ind. Microbiol. Biotechnol. 32, 301-308.

Bezman, S. A., Burtis, P. A., Izod, T. P. J., Thayer, M. A., 1978. Photodynamic inactivation of E. coli by rose bengal immobilized on polystyrene beads. Photochem. Photobiol. 28(3), 325-329.

Borkow, G., Gabbay, G., 2004. Putting copper into action: copper-

impregnated products with potent biocidal activities. FASEB J. 18, 1728-1730.

Boudaud, N., Machinal, C., David, F., Fréval-Le Bourdonnec, A., Jossent, J., Bakanga, F., Arnal, C., Jaffrezic, M. P., Oberti, S., Gantzer, C., 2012. Removal of MS2, Qβ and GA bacteriophages during drinking water treatment at pilot scale. Water Res. 46, 2651-2664.

Brame, J., Long, M., Li, Q., Alvarez, P., 2014. Trading oxidation power for efficiency: differential inhibition of photo-generated hydroxyl radicals versus singlet oxygen. Water Res. 60, 259-266.

Breijyeh, Z., Jubeh, B., Karaman, R., 2020. Resistance of Gram-negative bacteria to current antibacterial agents and approaches to resolve it. Molecules. 25, 1340.

Buonanno, M., Welch, D., Shuryak , I., Brenner, D. J., 2020. Far-UVC light (222 nm) efficiently and safely inactivates airborne human coronaviruses. Sci. Rep. 10. 10285.

Buonerba, A., Corpuz, M. Ballesteros F., Choo, K., Hasan S., Korshin, G., Belgiorno, V., Barceló, D., Naddeo, V., 2021. Coronavirus in water media: Analysis, fate, disinfection and epidemiological applications. J. Hazard. Mater. 415, 125580

Castro-Alférez, M., Polo-López, M. I., Fernández-Ibáñez, P., 2016. Intracellular mechanisms of solar water disinfection. Sci. Rep. 6(1), 38145.

Chen, L. Q., Kang, B., Ling, J., 2013. Cytotoxicity of cuprous oxide nanoparticles to fish blood cells: hemolysis and internalization. J.

Nanoparticle Res. 15, 1507.

Cho, M., Chung, H., Choi, W., Yoon, J., 2004. Linear correlation between inactivation of E. coli and OH radical concentration in TiO2 photocatalytic disinfection. Water Res. 38(4), 1069-1077.

Cho, M., Kim, J. H., Yoon, J., 2006. Investigating synergism during sequential inactivation of Bacillus Subtilis spores with several sisinfectants. Water Res. 40, 2911-2920.

Cho, M., Kim, J., Kim, J. Y., Yoon, J., Kim, J. H., 2010. Mechanisms of Escherichia Coli inactivation by several disinfectants. Water Res. 44, 3410-3418.

Cho, M., Lee, Y., Chung, H., Yoon, J., 2004. Inactivation of Escherichia coli by Photochemical Reaction of Ferrioxalate at Slightly Acidic and Near-Neutral pHs. Appl. Environ. Microbiol. 70(2), 1129-1134.

Cho, M., Chung, H., Choi, W., Yoon, J., 2005. Different Inactivation Behaviors of MS-2 Phage and Escherichia coli in TiO2 Photocatalytic Disinfection. Appl. Environ. Microbiol. 71(1), 270-275.

Cho, M., 2005. Doctoral dissertation, Seoul National University, Seoul, Korea.

Cho, M., Lee, J., Mackeyev, Y., Wilson, L. J., Alvarez, P. J. J., Hughes, J. B., Kim, J.-H., 2010. Visible Light Sensitized Inactivation of MS-2 Bacteriophage by a Cationic Amine-Functionalized C60 Derivative. Environ. Sci. Technol. 44(17), 6685-6691.

Crist, R. H., Oberholser, K., Schwartz, D., Marzoff, J., Ryder, D., Crist, D. L.

R., 1988. Interactions of metals and protons with algae. Environ. Sci. Technol. 22, 755−760.

Dahl, T. A., Midden, W. R., Hartman, P. E., 1987. Pure singlet oxygen cytotoxicity for bacteria. Photochem. Photobiol., 46(3), 345-352.

Dahl, T. A., Midden, W. R., Hartman, P. E., 1988. Comparison of killing of gram-negative and gram-positive bacteria by pure singlet oxygen. J. bacteriol. 171(4), 2188-2194.

Dahl, T. A., Midden, W. R., Hartman, P. E., 1989. Photochem. Photobiol., 48, 605.

Dow, S. M., Barbeau, B., Von Gunten, U., Chandrakanth, M., Amy, G., Hernandez, M., 2006. The impact of selected water quality parameters on the inactivation of Bacillus subtilis spores by monochloramine and ozone. Water Res. 40, 373-382.

Dwidjosiswojo, Z., Richard, J., Moritz, M. M., Dopp, E., Flemming, H. C., Wingender, J., 2011. Influence of copper ions on the viability and cytotoxicity of Pseudomonas aeruginosa under conditions relevant to drinking water environments. Int. J. Hyg. Environ. Health 214, 485-492.

Foote, C. S., 1968. Mechanisms of photosensitized oxidation: there are several different types of photosensitized oxidation which may be important in biological systems. Science. 162(3857), 963-970.

Foote, C. S., 1968. Photosensitized oxygenations and the role of singlet oxygen. Accounts Chem. Res. 1(4), 104-110.

Foster, H. A., Ditta, I .B., Varghese, S., Steele, A., 2011. Photocatalytic

disinfection using titanium dioxide: spectrum and mechanism of antimicrobial activity. Appl. Microbiol. Biotechnol. 90(6), 1847-1868.

Gomes, I. B., Simões, M., Simões, L. C., 2016. The effects of sodium hypochlorite against selected drinking water-isolated bacteria in planktonic and sessile states. Sci. Total Environ. 565, 40-48.

Gunten, U. V., 2003. Ozonation of drinking water: Part I. Oxidation kinetics and product formation. Water Res. 37. 1443-1467.

Gunten, U. V., 2003. Ozonation of drinking water: Part II. Disinfection and by-product formation in presence of bromide, iodide or chlorine. Water Res. 37. 1469-1487.

Helgason, E., Økstad, O. A., Caugant, D. A., Johansen, H. A., Fouet, A., Mock, M., Hegna, I., Kolstø, A. B. 2000. Bacillus anthracis, Bacillus cereus, and bacillus thuringiensis - One species on the basis of genetic evidence. Applied and Environmental Microbiology, 66(6).

Horie, Y., David, D. A., Taya, M., Tone, S., 1996. Effects of light intensity and titanium dioxide concentration on photocatalytic sterilization rates of microbial cells. Ind. Eng. Chem. Res. 35(11), 3920-3926.

Hotze, E. M., Badireddy, A. R., Chellam, S., Weisner, M. R., 2009. Mechanisms of Bacteriophage Inactivation via Singlet Oxygen Generation in UV Illuminated Fullerol Suspensions. Environ. Sci. Technol. 43(17), 6639-6645.

How, Z. T., Busetti, F., Linge, K. L., Kristiana, I., Joll, C. A., Charrois, J. W. A. 2014. Analysis of free amino acids in natural waters by liquid chromatography–tandem mass spectrometry. J. Chromat. A, 1370, 135–146.

Hunt, N. K., and Mariñas, B. J., 1997. Kinetics of Escherichia coli inactivation with ozone. Water Res. 31(6), 1355-1362.

Inglesby, T. v., Dennis, D. T., Henderson, D. A., Bartlett, J. G., Ascher, M. S., Eitzen, E., Fine, A. D., Friedlander, A. M., Hauer, J., Koerner, J. F., Layton, M., McDade, J., Osterholm, M. T., O'Toole, T., Parker, G., Perl, T. M., Russell, P. K., Schoch-Spana, M., Tonat, K. 2000. Plague as a biological weapon: Medical and public health management. JAMA, 283(17).

Jiménez-Hernández, M. E., Manjón, F., García-Fresnadillo, D., Orellana, G., 2006. Solar water disinfection by singlet oxygen photogenerated with polymer-supported Ru (II) sensitizers. Sol. Energy. 80(10), 1382-1387.

Kim, H. -E., Lee, H. -J., Kim, M. S., Kim, T., Lee, H., Kim, H. -H., Cho, M., Hong, S. -W., Lee, C., 2019. Differential microbicidal effects of bimetallic iron–copper nanoparticles on Escherichia coli and MS2 Coliphage. Environ. Sci. Technol. 53, 2679-2687.

Kim, H. -E., Nguyen, T. T. M., Lee, H., Lee, C., 2015. Enhanced inactivation of Escherichia coli and MS2 Coliphage by cupric ion in the presence of hydroxylamine: Dual microbicidal effects. Environ. Sci. Technol. 49, 14416-14423.

Kim, T., Kim, H. -E., Cho, J., Kim, H. -H., Seo, J., Lee, J., Choi, J. Y., Lee, C., 2019. Inactivation of Escherichia Coli and MS2 Coliphage via singlet

oxygen generated by homogeneous photosensitization. Korean J. Chem. Eng. 36, 1785-1790.

Kirakosyan, G., Trchounian, K., Vardanyan, Z., Trchounian, A., 2008. Copper (II) ions affect Escherichia Coli membrane vesicles' SH-Groups and a disulfide-dithiol interchange between membrane proteins. Cell Biochem. Biophys. 51, 45-50.

Kohn, T., and Nelson, K. L., 2007. Sunlight-mediated inactivation of MS2 coliphage via exogenous singlet oxygen produced by sensitizers in natural waters. Environ. Sci. Technol. 41(1), 192-197.

Kouame, Y., and Haas, C. N., 1991. Inactivation of E. coli by combined action of free chlorine and monochloramine. Water Res. 25(9), 1027-1032.

Kuzmanovic, D. A., Elashvili, I., Wick, C., O'Connell, C., Krueger, S., 2006. The MS2 coat protein shell is likely assembled under tension: A novel role for the MS2 bacteriophage a protein as revealed by small-angle neutron scattering. J. Mol. Biol. 355, 1095-1111.

Lee, H., Lee, H. J., Seo, J., Kim, H. E., Shin, Y. K., Kim, J. H., Lee, C., 2016. Activation of oxygen and hydrogen peroxide by copper(II) coupled with hydroxylamine for oxidation of organic contaminants. Environ. Sci. Technol. 50, 8231-8238.

Lee, H. -J., Kim, H. -E., Lee, C., 2017 Combination of cupric ion with hydroxylamine and hydrogen peroxide for the control of bacterial biofilms on RO membranes. Water Res. 110, 83-90.

Leiman, P. G., Kanamaru, S., Mesyanzhinov, V. V., Arisaka, F., Rossmann,

M. G., 2003. Structure and morphogenesis of bacteriophage T4. Cell. Mol. Life Sci. 60, 2356-2370.

Liu, C., Kong, D., Hsu, P. C., Yuan, H., Lee, H. W., Liu, Y., Wang, H., Wang, S., Yan, K., Lin, D., Maraccini, P. A., Parker, K. M., Boehm, A. B., Cui, Y., 2016. Rapid water disinfection using vertically aligned MoS2 nanofilms and visible light. Nat. Nanotechnol. 11(12), 1098-1104.

Liu, J., Zhang, T., Lu, T., Qu, L., Zhou, H., Zhang, Q., Ji, L., 2002. DNA-Binding and cleavage studies of macrocyclic copper(II) complexes. J. of Inorg. Biochem. 91, 269-276.

Luo, L. W., Wu, Y. H., Yu, T., Wang, Y. H., Chen, G. Q., Tong, X., Bai, Y., Xu, C., Wang, H. bin, Ikuno, N., Hu, H. Y. 2021. Evaluating method and potential risks of chlorine-resistant bacteria (CRB): A review. Water Research, 188, 116474.

Mamane, H., Shemer, H., Linden, K. G., 2007. Inactivation of E. coli, B. subtilis spores, and MS2, T4, and T7 phage using UV/H2O2 advanced oxidation. J. Hazard. Mater. 146(3), 479-486.

Maness, P. C., Smolinski, S., Blake, D. M., Huang, Z., Wolfrum, E. J., Jacoby, W. A., 1999. Bactericidal activity of photocatalytic TiO_2 Reaction: Toward an understanding of its killing mechanism. Appl. Environ. Microbiol. 65, 4094-4098.

Møretrø, T., Heir, E., Nesse, L. L., Vestby, L. K., Langsrud, S., 2012. Control of salmonella in food related environments by chemical disinfection. Food Res. Int. 45, 532-544.

Müller-Breitkreutz, K., Mohr, H., Brivida, K., Seis, H., 1995. Inactivation of viruses by chemically and photochemically generated singlet molecular oxygen. J. Photoch. Photobio. B-Biol. 30(1), 63-70.

Müller, D. J., and Engel, A., 1999. pH and voltage induced structural changes of porin OmpF explain channel closure. J. Mol. Biol. 285(4), 1347-1351.

Nguyen, T. T. M., Park, H. -J., Kim, J. Y., Kim, H. -E., Lee, H., Yoon, J., Lee, C., 2013. Microbial inactivation by cupric ion in combination with H_2O_2: Role of reactive oxidants. Environ. Sci. Technol. 47 (23), 13661−13667.

Ohsumi, Y., Kitamoto, K., Anraku, Y., 1988. Changes induced in the permeability barrier of the yeast plasma membrane by cupric Ion. J. Bacteriol. 170, 2676−2682.

Park, S. Y., and Kim, C. G., 2018. A comparative study of three different viability tests for chemically or thermally inactivated Escherichia coli. Environ. Eng. Res. 23(3), 282-287.

Park, H. -J., Nguyen, T. T. M., Yoon, J., Lee, C., 2012. Role of reactive oxygen species in Escherichia Coli inactivation by cupric ion. Environ. Sci. Technol. 46 (20), 11299−11304.

Park, J. -A., Kang, J. -K., Kim, J. -H., Kim, S. -B., Yu, S., Kim, T. -H., 2015. Bacteriophage removal in various clay minerals and clay-amended soils. Environ. Eng. Res. 20, 133-140.

Pankuweit, s., Ristić, A. D., Seferović, P. M., Maisch, B., 2005, Bacterial

Pericarditis. Am. J. Cardiovasc. Drugs. 5,103-112

Polk, D. B., Peek, R. M., Helicobacter pylori: gastric cancer and beyond. Nat. Rev. Cancer. 10, 403-414

Rajendirn, V., Karthik, R., Palaniandavar, M., Stoeckli-Evans, H., Periasamy, V. S., Akbarsha, M. A., Srinag, B. S. Krishnamurthy, H., 2007. Mixed-ligand copper (II)-phenolate complexes: effect of coligand on enhanced DNA and protein binding, DNA cleavage, and anticancer activity. Inorg. Chem. 46, 8208-8221.

Rennecker, J. L., Mariñas, B. J., Owens, J. H., Rice, E. W., 1999. Inactivation of Cryptosporidium parvum oocysts with ozone. Water Res. 33(11), 2481-2488.

Ryberg, E., Chu, C., Kim, J. -H., 2018. Edible Dye-Enhanced Solar Disinfection with Safety Indication. Environ. Sci. Technol. 52(22), 13361-13369.

Schäfer, M., Schmitz, C., Facius, R., Horneck, G., Milow, B., Funken, K. -H., Ortner, J., 2000. Systematic study of parameters influencing the action of rose bengal with visible light on bacterial cells: comparison between the biological effect and singlet-oxygen production. Photochem. Photobiol. 71(5), 514-523.

Scully, F. E. Jr and Hoigné, J., 1987. Rate constants for reactions of singlet oxygen with phenols and other compounds in water. Chemosphere. 16(4), 681-694.

Shin, G. A., Sobsey, M. D., 2003. Reduction of Norwalk virus, poliovirus 1, and bacteriophage MS2 by ozone disinfection of water. Appl. Environ. Microbiol. 69, 3975-3978.

Silverman, A. I., Peterson, B. M., Boehm, A. B., McNeill, K., Nelson, K. L., 2013. Sunlight Inactivation of Human Viruses and Bacteriophages in Coastal Waters Containing Natural Photosensitizers. Environ. Sci. Technol. 47(4), 1870-1878.

Sobsey, M. D., 1989. Inactivation of health-related microorganisms in water by disinfection processes. Water Sci. Technol. 21, 179-195.

Sohn, J., Amy, G., Cho, J., Lee, Y., Yoon, Y., 2004. Disinfectant decay and disinfection by-products formationmodel development: chlorination and ozonation by-products. Water Res. 38, 2461-2478.

Sproul, O. J., Pfister, R. M., Kim, C. K., 1982. The mechanism of ozone inactivation of water borne viruses. Water Sci. Technol. 14, 303-314.

Vandermeulen, G., Marie, C., Scherman, D., Préat, V. 2011. New Generation of Plasmid Backbones Devoid of Antibiotic Resistance Marker for Gene Therapy Trials. Molecular Therapy, 19(11), 1942–1949.

Venczel, L.., Arrowood, M., Hurd, M., Sobsey, M. D. 1997. Inactivation of Cryptosporidium parvum oocysts and Clostridium perfringens spores by a mixed-oxidant disinfectant and by free chlorine. Appl. Environ. Microbiol., 63(4).

Viles, J. H., Cohen, F. E., Prusiner, S. B., Goodin, D. B., Wright, P. E., Dyson, H. J., 1999. Copper binding to the prion protein: Structural

implications of four identical cooperative binding sites. Proc. Natl. Acad. Sci. USA 96, 2042-2047.

Wang, J., Shen, J., Ye, D., Yan, X., Zhang, Y., Yang, W., Li, X., Wang, J., Zhang, L., Pan, L., 2020. Disinfection technology of hospital wastes and wastewater: Suggestions for disinfection strategy during coronavirus Disease 2019 (COVID-19) pandemic in China. Environ. pollut. 262, 114665

entworth, B. B., and French, L., 1970. Plaque assay of cytomegalovirus strains of human origin. Exp. Biol. Med. 135(2), 253-258.

Young, S. B., Setlow, P., 2003. Mechanisms of killing of Bacillus subtilis spores by hypochlorite and chlorine dioxide. J. Appl. Microbiol. 95, 54-67.

Zou, S., Guo, J., Gao, R., Dong, L., Zhou, J., Zhang, Y., Dong, J., Bo, H., Qin, K., Shu, Y., 2013. Inactivation of the novel avian influenza A (H7N9) virus under physical conditions or chemical agents treatment. Virol. J. 10, 289.

Abstract

최근 다양한 병원균의 창궐과 감염사고로 인하여 소독에 대한 필요성이 지속적으로 증가하고 있다. 특히 공기를 매개로 전파하는 특정 바이러스 종 들의 감염경로가 다양해지면서 물을 통해 전파될 가능성이 제기된 바 있어 물 속 병원균 불활성화에 관한 관심이 전세계적으로 크게 늘었다. 물 속 병원균을 제어하기 위해서는 염소, 오존 등의 화학적 산화방법과 광화학적 소독시스템을 적용할 수 있다.

본 연구에서는 소독공정에서 적용되는 다양한 소독제와 미생물 쌍의 불활성화 효율을 정량적으로 해석하고자 하였고, 그 불활성화 기작에 대해서 규명하고자 하였다. 소독제로는 광화학적 소독제인 단일항산소와 화학적 소독제인 염소, 오존 그리고 과산화수소, 그리고 구리계 소독시스템을 적용하였다. 미생물로는 대장균을 비롯한 박테리아 8종(병원성 2종 포함)과 박테리오 파지 4종, 병원성 바이러스(공기매개 전파) 2종을 선택하였으며 각 미생물 별로 한 종이상의 소독공정을 적용하여 각 소독공정의 효율을 비교하였다. 추가적으로 병원성 바이러스에 대해서는 불활성화 기작을 일반화하는 연구를 추가적으로 수행하여 불활성화 기여도를 나타내었다. 주요 결과는 아래와 같다.

첫째, 광화학적 소독시스템에 의해 생성된 단일항산소는 미생물의 불활성화와 선형의 상관관계를 나타내며 박테리아에 비해 바이러스에서 높은 불활성화 효율을 나타낸다.

둘째, 구리계 소독시스템의 적용을 통해 미생물의 구조적 특징으로 분류하였을때, 미생물 불활성화의 경향성의 유사도가 높아진 다는 것

을 확인하였으며, 이 구조적 특징은 펩티도글리칸 층의 두께, 유전물질의 가닥 수 등을 포함한다.

셋째, 기존 소독제를 활용하여도 공기매개 전염 병원균의 불활성화는 쉽게 가능하나, 상대적으로 불활성화 효율이 낮다는 점을 확인하였다. 추가적으로 미생물의 불활성화 효율은 단순히 산화제의 종류와 농도에 의하여 결정되는 것이 아닌 pH에 의한 구조체의 변화 등을 동시에 적용하여 예측하여야 한다는 점을 확인하였다.